In the bone marrow (BM), Wnt proteins activate the beta-catenin pathway and the non-obese severe combined immunodeficient (NOD-SCID)-repopulating capacity of normal haematopoietic stem cells. They lead to increased expression of *HOXB4* and *NOTCH1* implicated in the self-renewal of haematopoietic stem cells (Reya *et al*, 2003). Up-regulation of the beta-catenin pathway has been suggested in chronic myeloid leukaemia (CML)-derived granulocyte-macrophage progenitor cells (GMPs) and multiple myeloma (MM) cells (Derksen *et al*, 2004; Jamieson *et al*, 2004). Furthermore, beta-catenin reportedly plays a significant role in promoting cell proliferation, adhesion, and survival *in vitro* (Chung *et al*, 2002). The expression of beta-catenin is also enhanced by oncogenic FLT3 signals and associated with poor prognosis (Tickenbrock *et al*, 2005; Ysebaert *et al*, 2006). However, there are some contradictory reports. Studies of conditional knock-out mice with a beta-catenin gene (*Ctnnb1*) deletion indicated that *Ctnnb1* is not indispensable for haematopoiesis (Cobas *et al*, 2004). Furthermore, an active form of *Ctnnb1* compromised haematopoietic stem cell maintenance and blocked differentiation in transgenic mice experiments (Simon *et al*, 2005). The role of the Wnt/beta-catenin pathway in malignant haematopoiesis therefore needs to be further elucidated.

According to previous studies, the expression of beta-catenin is associated with activation of the Wnt pathway as well as poor prognosis (Tickenbrock *et al*, 2005; Ysebaert *et al*, 2006). However, beta-catenin is associated not only with Wnt signaling but also with adherence junctions (Conacci-Sorrell *et al*, 2002). It is anchored to the cell inner surface membrane via cadherins. In normal bone marrow (BM), the vascular endothelium expresses a significantly higher amount of beta-catenin relative to the level in haematopoietic cells. Accordingly, immunohistochemical detection of nuclear NPBC would enable a better understanding of the role of beta-catenin in leukaemia.

This study investigated the subcellular localization of beta-catenin in BM specimens from acute myeloid leukaemia (AML) and myelodysplastic syndrome (MDS) patients using two anti-beta-catenin antibodies: one against C-terminal peptides and another against N-terminal non-phosphorylated peptides. The latter antibody detected nuclear NPBC, and positive staining for nuclear NPBC was associated with particular clinical characteristics of AML and MDS.

Table I. Clinical characteristics of AML and MDS patients according to nuclear NPBC expression.

	Nuclear NPBC$^+$	Nuclear NPBC$^-$	*P*-value
Patients with *de novo* AML	22	32	
Age (median)	54 (20–81)	53 (18–71)	NS
Sex/male/female	18/4	17/15	0·005
Laboratory data			
WBC ($\times10^9$/l; median)	3·5 (0·8–92·5)	5·3 (0·7–202·1)	NS
Hb (g/l; median)	74 (43–134)	98 (36–141)	0·01
PLT ($\times10^9$/l; median)	7·6 (0·3–170)	4·2 (1·1–27·3)	NS
PB blasts (%; median)	24 (0–82)	39 (0–99)	NS
BM blasts (%; median)	46·2 (20–86·5)	77·5 (29–98)	0·02
CR rate	13/22 (59·1%)	24/27 (88·9%)	0·01
Relapse rate	16/21 (76·2%)	14/24 (58·3%)	0·03
Patients with MDS	18	26	
Age	59 (26–76)	57 (22–89)	
Sex/male/female	12/6	16/10	0·05
Laboratory data			
WBC ($\times10^9$/l; median)	2·9 (1·2–9·0)	2·6 (1·6–5·9)	NS
Hb (g/l; median)	75 (46–151)	85 (47–127)	NS
PLT ($\times10^9$/l; median)	79 (7–122)	44 (7–400)	NS
BM blasts (%; median)	3 (0–30)	5 (0–30)	NS
IPSS score*			
Low risk	0	4	NS
Intermediate-1	4	12	NS
Intermediate-2	4	4	NS
High risk	3	1	0·04

NPBC, non-phosphorylated beta-catenin; AML, acute myeloid leukaemia; MDS, myelodysplastic syndrome; WBC, white blood cell count; Hb, hemoglobin concentration; PLT, platelet count; PB, peripheral blood; BM, bone marrow; CR, complete remission; IPSS, International Prognostic Scoring System.

*Full data was available in 32 of the 44 patients with MDS.

Materials and methods

Patient samples

For clinical samples, BM clots were obtained during routine diagnostic procedures. Beta-catenin expression was analyzed in BM specimens from patients newly diagnosed at the Nagoya University Hospital between 2000 and 2006 (Table I). The *de novo* AML patients consisted of 35 men and 19 women with a median age of 53 years (range, 20–81 years), and *FLT3* mutations were detected in seven of 22 patients with AML (31·8%). The MDS patients consisted of 28 men and 16 women with a median age of 57 years (range, 22–89 years). BM mononuclear cells were harvested by standard Ficoll/Paque density gradient centrifugation (Amersham Pharmacia Biosciences, Roozendaal, the Netherlands), and were suspended in RPMI 1640 medium supplemented with 10% fetal bovine serum, 100 IU/ml of penicillin G and 100 μg/ml of streptomycin.

Antibodies

For immunohistochemical and immunoblot studies, two monoclonal antibodies were used; one was against C-terminal peptides (clone14, IgG1; BD Transduction Laboratories/Life Science Research, Heidelberg, Germany), enabling recognition of pan beta-catenin (PBC), and the other was against

N-terminal-peptides (clone 8E4, IgG1; Alexis Biochemicals, Lausanne, Switzerland), enabling recognition of NPBC.

Immunohistochemical staining

Samples were fixed with ice-cold 4% paraformaldehyde for 16–24 h, embedded in paraffin, sectioned transversely (thickness, 3 μm), and processed for immunohistochemistry to determine the localization of beta-catenin. After removal of paraffin with xylene and dehydration with a series of ethanol solutions, the tissue sections were subjected to microwave irradiation (750 W) for 15 min in 0·01 mol/l citrate buffer (pH 6·0). The sections were then placed in an automated immunostainer (Ventana Medical Systems, Tucson, AZ, USA) as described (Xu *et al*, 2002). For negative controls, primary antibodies were replaced with mouse IgG. The subcellular distribution of beta-catenin (i.e. restriction to the nucleus or presence in the membrane) was assessed without knowledge of the French-America-British (FAB) subtypes, *FLT3* mutations or karyotypes. We investigated a single case twice for NPBC expression. The entire section was screened to find the region with the highest immunostaining. The score was determined in each case after counting at least 500 nuclei in 3–5 randomly selected regions. When 20% or more of the BM mononuclear cells were positive for nuclear staining of NPBC, they were classified as nuclear NPBC$^+$. The cut-off value of 20% was determined by the median distribution of the percentage of BM mononuclear cells stained by NPBC. As described in the results, some erythroblasts were positive for NPBC but the number was <20% except in the case of M6 patients. On the other hand, almost all blasts in M7 and other cases tested positive. The discrimination of cell types based on the 20% criterion therefore enabled a clear delineation.

Immunoblotting

Cell lysates from AML cells were extracted as previously described (Ozeki *et al*, 2004). A total of 1×10^6 cells were directly lysed in sample buffer and then subjected to sodium dodecyl sulphate-polyacrylamide gel electrophoresis on a 10% gel, and the separated proteins were transferred to a polyvinylidene difluoride membrane (Bio-Rad, Hercules, CA, USA). The membrane was initially incubated at room temperature for 1 h with 5% nonfat milk and 0·1% Tween-20 in Tris-buffered saline and then overnight with mouse monoclonal antibodies at a 1:2000 dilution in the same solution. After washing, the membrane was incubated for 1 h with a 1:5000 dilution of horseradish peroxidase-conjugated mouse antibodies to mouse IgG (MBL, Amersham, Bucks, UK), and immune complexes were then detected with enhanced chemiluminescence (ECL) reagents (Amersham).

Statistical analysis

The χ^2 test was used to calculate the difference of frequencies between nuclear NPBC$^+$ and NPBC$^-$ groups. The Mann–Whitney *U*-test was used to compare continuous variables. Kaplan–Meier curves were drawn using STATVIEW software (Macintosh; SAS Institute, Cary, NC, USA). *P*-values <0·05 were considered significant.

Results

Using an anti-beta-catenin C-terminal peptide antibody, beta-catenin was stained in the membrane and cytoplasm of erythroid cells from normal BM. In *de novo* AML specimens, significant staining was observed only in M6. This antibody also detected BM vessels whose density was increased in AML specimens as previously reported (Serinsöz *et al*, 2004; Fig 1A). On the other hand, an anti-N-terminal nonphosphorylated peptide antibody gave no significant staining in the normal BM. In AML specimens, nuclear NPBC was detected in erythroid blasts, megakaryoblasts and some myeloblasts (Fig 1A). In M6 specimens, nuclear NPBC was detected in 30–80% of myelomonocytic cells and nearly 100% of erythroblastic cells (Fig 1A). In M7 specimens, megakaryocytes were also strongly positive for nuclear NPBC (Fig 1A). In total, 20% or more of the BM mononuclear cells were positive for nuclear NPBC in 22 (40·7%) of 54 AML patients (Table I, Fig 1B). There was a strong male predominance of nuclear NPBC$^+$ cases, comprising 81·8% (18/22) in AML patients (Table I). However, the reason for this is unclear. In our cohort study, the karyotypes of female patients correlated to t(8;21)/t(15;17), which did not express nuclear NPBC. Thus the small numbers of studied patients seem to give some bias to the male predominance. A large-scale study is necessary to confirm this association. Nuclear NPBC$^+$ staining was closely associated with AML subtype: it occurred frequently (8/9) in M6 and M7 and rarely (0/7) in M3 (Fig 1B), and nuclear NPBC$^+$ was preferentially detected in erythroid and megakaryoblastic leukaemia compared to other myeloid leukaemias (M6–M7 vs. M0–M5, $P < 0·001$).

In MDS specimens, erythroid cells and endothelial cells were stained with the anti-beta-catenin C-terminal peptide antibody (Fig 2A). As observed for AML specimens, the cytoplasm and inner membrane were stained by this antibody. The anti-beta-catenin N-terminal nonphosphorylated peptide antibody detected nuclear staining in myeloblasts and erythroblasts that was similar to the pattern seen in AML cases (Fig 2A). Nuclear NPBC was found in 18 (40·9%) of 44 MDS patients, and was related to the FAB classification of MDS (Table I, Fig 2B). Nuclear NPBC$^+$ was preferentially detected in refractory anaemia with excess blasts in transformation (RAEBT) compared to other MDS subtypes [RAEBT *versus* refractory anaemia (RA)/refractory anaemia with ringed sideroblasts (RARS)/RAEB, $P = 0·01$].

To confirm whether these two antibodies recognized beta-catenin, a total of 41 samples from AML and MDS patients were subjected to immunoblot analysis. The anti-beta-catenin C-terminal peptide antibody detected bands at a molecular weight of 95 kDa, corresponding to beta-catenin, in most

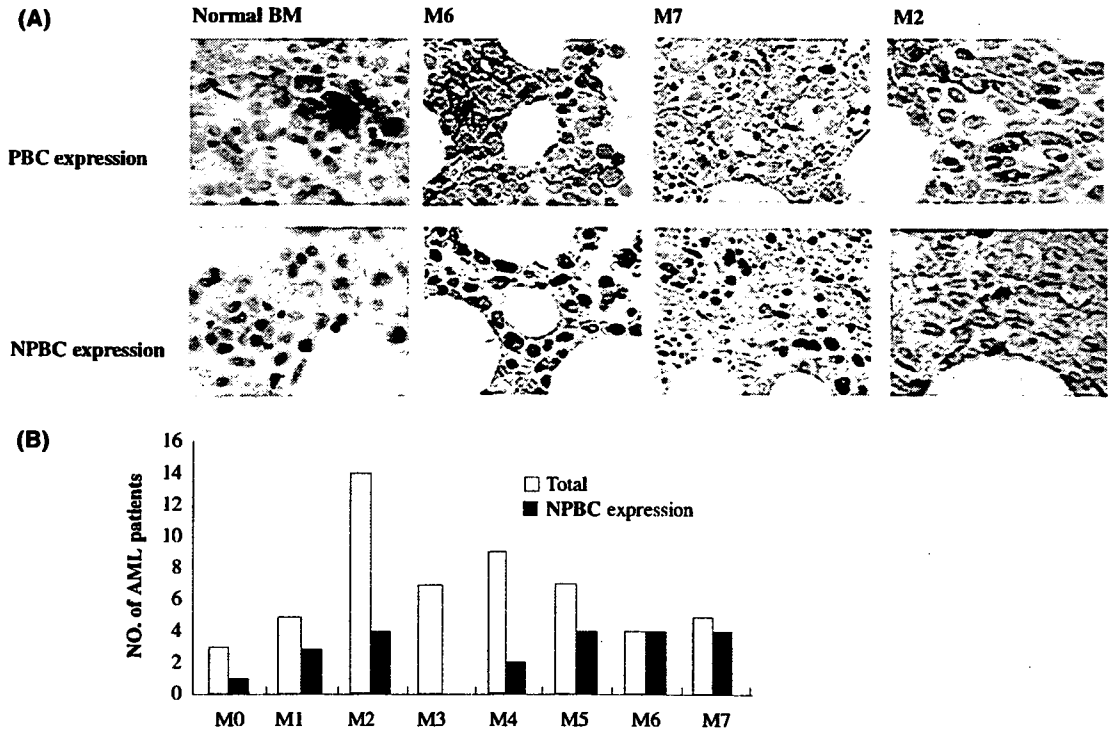

Fig 1. Specific association of NPBC expression with FAB subtypes of AML specimens. (A) In normal BM clots, PBC is expressed on the membranes of erythroid cells as well as endothelial cells. NPBC was not detected in normal BM clots. Most erythroid cells and endothelial cells showed cell membrane expression of PBC without expression in the nucleus or cytoplasm. NPBC was expressed in leukemia cells and was always restricted to the nucleus, especially in M6 and M7 specimens. Prominent staining of endothelial cells was seen in the vascular tissue in BM derived from an M2 patient with, though NPBC staining was negative in the same specimen. Original magnification ×40. (B) The graph presents data based on nuclear NPBC staining in paraffin sections from 54 patients with AML.

samples except for M3 (Fig 3A). The anti-N-terminal nonphosphorylated peptide antibody gave bands of the same size in only a few samples of AML and MDS (Fig 3B). The results of immunoblotting corresponded to those of immunostaining, although the latter was more sensitive than the former.

The above findings suggest that expression of nuclear NPBC could be used to identify some subsets of AML and MDS. Next we studied whether nuclear NPBC was associated with chromosomal abnormalities or genetic alterations. Previous studies suggested that AML-associated translocations, such as t(8;21) and t(15;17), contributed to the activation of gamma-catenin, or that *FLT3* mutation might be associated with the stabilization of beta-catenin. In this study, however, nuclear NPBC was never detected in AML with t(8;21) or t(15;17). In AML/MDS with −7/−7q and a complex karyotype, nuclear NPBC was frequently detected ($P = 0{\cdot}007$ and $P = 0{\cdot}02$, respectively; Table II). Moreover, detection was not related to *FLT3* internal tandem duplication (ITD; Table II).

Finally, we studied whether clinical characteristics and outcome were different between nuclear NPBC$^+$ and NPBC$^-$ AML patients. NPBC$^+$ AML patients showed significantly lower hemoglobin levels, lower blast percentages in the BM, and lower CR rates (Table I). There were no significant differences between the NPBC$^+$ and NPBC$^-$ groups in the MDS patients (Table I). However, nuclear NPBC was associated with a high International Prognostic Scoring System (IPSS) score (Table I). Of note, nuclear NPBC$^+$ AML patients had worse overall survival than NPBC$^-$ AML patients (Fig 4A). Even if the M6/M7 subtype and/or M3 subtype was excluded from the analysis, there was still a significant association between nuclear NPBC$^+$ and survival (Fig 4B–D).

Discussion

This study used nuclear NPBC as a biomarker for the activated Wnt/beta-catenin signaling pathway. The anti-beta-catenin C-terminal peptide antibody detected total beta-catenin in immunoblots but mainly cytoplasmic and membrane-associated beta-catenin in immunohistological analysis, whereas the anti-beta-catenin N-terminal nonphospholylated peptide antibody detected only nuclear beta-catenin in both analyses (data not shown). Accordingly, it was concluded that the nuclear staining with the latter antibody identified nuclear nonphosphorylated beta-catenin. Nuclear NPBC was detected in 22 (40·7%) of 54 AML patients and 18 (40·9%) of 44 MDS patients. Positive staining of nuclear NPBC was associated with particular AML subtypes (M6 and M7), a low complete remission rate, and poor prognosis. The presence of nuclear

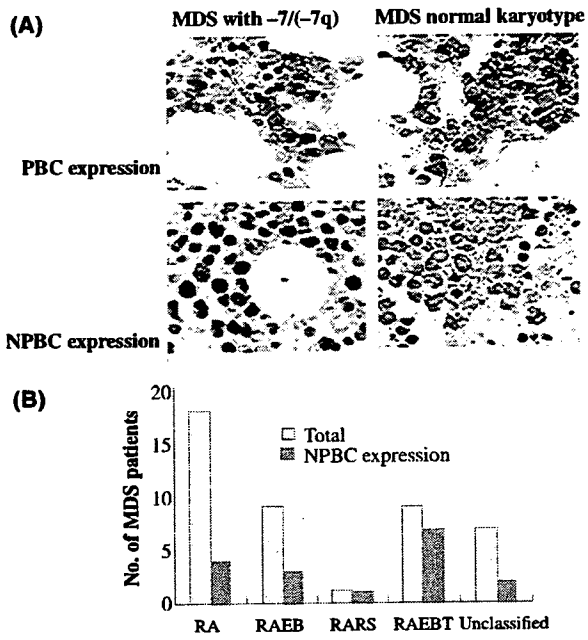

Fig 2. Specific association of NPBC expression with FAB subtypes of MDS specimens. (A) Most erythroid cells and endothelial cells showed cell membrane expression of PBC without expression in the nucleus or cytoplasm. NPBC was expressed in erythroid cells and was always restricted to the nucleus, especially in refractory anaemia with excess blasts in transformation (RAEBT) and MDS specimens with −7/−7(q). Original magnification ×40. (B) The graph presents data obtained for nuclear NPBC staining in paraffin sections from 44 patients with MDS. RA, refractory anaemia; RARS, RA with ringed sideroblasts; RAEB, RA with excess blasts.

NPBC was also associated with a high IPSS score of MDS and with −7/−7q and complex karyotypes.

Previous reports indicated that a significant proportion of AML samples expressed beta-catenin on immunoblot analysis.

Table II. Cytogenetic abnormalities and *FLT3* mutation according to nuclear NPBC expression.

	Nuclear NPBC$^+$ (*N*)	Nuclear NPBC$^-$ (*N*)	*P*-value
Karyotypes			
t(8;21)	0	3	NS
t(15;17)	0	4	NS
−5/−5q	4	1	NS
−7/−7q	12	6	0·007
Complex	13	7	0·02
Others	19	2	NS
Normal	10	31	0·0003
Unknown	7	1	0·02
FLT3 mutation			
Wild type	3	12	0·006
ITD	2	5	NS

Patients are counted more than once due to the coexistence of more than one cytogenetic abnormality. Complex patients had three or more cytogenetic abnormalities.
NPBC, non-phosphorylated beta-catenin; ITD, internal tandem repeat; NS, not significant.

The expression of beta-catenin is related to CD34 expression, poor prognosis and clonogenic capacity *ex vivo* (Ysebaert *et al*, 2006). Furthermore, beta-catenin is expressed in normal CD34$^+$ progenitor cells and the expression level is reduced upon differentiation (Simon *et al*, 2005). In these studies, however, the total beta-catenin level was analyzed only by immunoblot analysis. Beta-catenin is expressed not only as nuclear NPBC but also as a cadherin-associated protein in the inner cytomembrane (Conacci-Sorrell *et al*, 2002). The present study found that normal erythroblasts expressed cytoplasmic or membrane-associated beta-catenin but not nuclear NPBC (Fig 1A). Both membrane-associated and nuclear beta-catenin was expressed in malignant erythroblasts in subtype M6

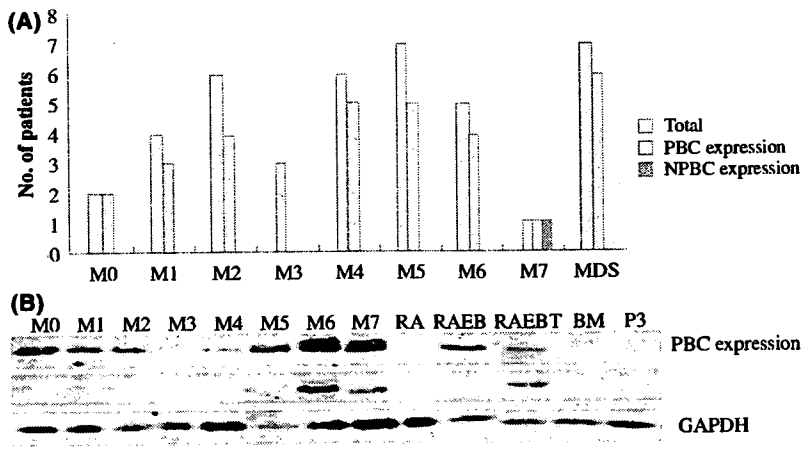

Fig 3. Beta-catenin expression of AML cells assessed by immunoblotting. (A) The graph shows data obtained for the expression of NPBC in mononuclear cells from 41 patients with AML, and the data indicate that expression of NPBC is specific to some FAB subtypes, especially to M6 and M7. (B) Representative immunoblots for PBC and NPBC in AML samples. RA, refractory anaemia; RARS, RA with ringed sideroblasts; RAEB, RA with excess blasts; RAEBT, refractory anaemia with excess blasts in transformation.

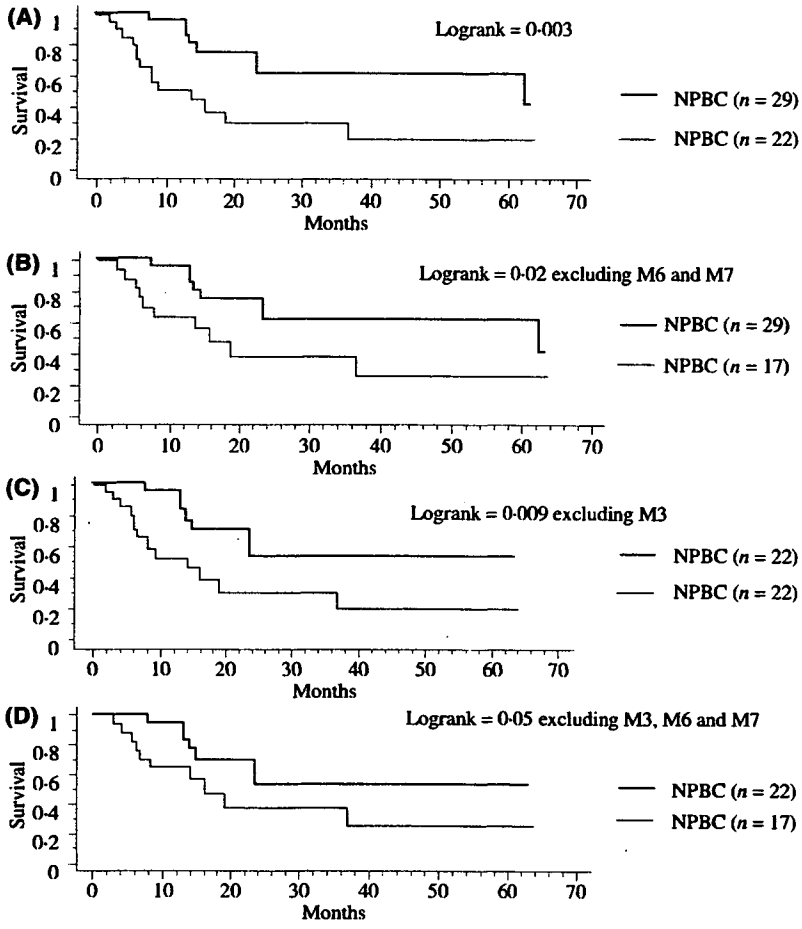

Fig 4. Kaplan–Meier cumulative survival curves were calculated for 51 AML patients (A) and 46 patients excluding subtype M6/M7 (B), 44 patients excluding subtype M3 (C), 39 patients excluding subtype M3/M6/M7 (D), respectively, according to the presence of nuclear NPBC. Comparison of the survival curves using the log-rank test identified nuclear NPBC$^+$ as a prognostic factor.

(Fig 1A). These findings suggest that increased nuclear NPBC levels were the result of aberrant signal transduction in the Wnt pathway or an abnormality of beta-catenin itself.

In this study, the expression levels of total and non-phosphorylated beta-catenin were correlated but varied significantly among leukemia samples. In M6 and M7 samples, the expression of beta-catenin was significantly augmented, whereas it was hardly detected in M3 and normal BM samples. These variations suggest the possibility that Wnt/beta-catenin signaling is mediated by multiple factors, such as immaturity, lineage, and oncogenic signals.

We established a correlation between nuclear NPBC$^+$ and poor survival in AML patients. The prognostic value of total beta-catenin expression has been previously studied in AML patients (Ysebaert *et al*, 2006), but the present study clearly showed for the first time that nuclear NPBC is associated with prognosis. The association was still observed even if M6/M7 and/or M3 patients were excluded from the analysis. Nuclear NPBC might be a new prognostic marker for AML and MDS that can be evaluated by histopathological examination.

Wnts are a family of paracrine and autocrine factors that regulate cell growth and cell fate (Reya *et al*, 2003). The Wnt autocrine signaling mechanism was initially discovered in human breast and ovarian tumor cell lines as well as in MM primary samples (Bafico *et al*, 2004; Derksen *et al*, 2004). Since several Wnt family members have been reported in BM stromal cells, it is possible that leukaemia cells respond to different proteins of the Wnt/beta-catenin pathway secreted by stromal cells in a paracrine fashion (Austin *et al*, 1997; Van Den Berg *et al*, 1998; Etheridge *et al*, 2004). Nuclear NPBC was detected in some cell lines only when they were transplanted in non-obese diabetic/severe combined immunodeficient/gammacnull (NOG) mice (data not shown). Thus, the leukaemia niche may have an important role in nuclear NPBC expression during AML.

MDS is a clonal hematopoietic stem cell disorder characterized by multi-lineage dysplasia and pancytopenia in which further genetic events may be required for the rapid expansion of leukaemic blasts (Heaney & Golde, 1999; Hirai, 2003). Although nuclear NPBC has been studied in many cancers as

well as haematological malignancies, it has not been studied in MDS (Morin *et al*, 1997; Barker & Clevers, 2000; Giles *et al*, 2003). This is the first study to report the expression of beta-catenin in MDS patients. Here we showed that nuclear NPBC was related to the IPSS score and that secondary AML from MDS showed the highest percentage of nuclear NPBC expression. The Wnt signaling pathway may play an important role in the pathogenesis of the transformation of MDS into AML. Regarding chromosomal abnormalities, −7/−7q and/or complex karyotypes were significantly associated with the presence of nuclear NPBC. According to recent data (Liu *et al*, 2006), the gene encoding alpha-catenin (*CTNNA1*) is suppressed by deletion and/or methylation. Both alpha-catenin and beta-catenin bind to the inner membrane of hematopoietic cells, and cadherin binds to actin filaments via the catenin complex. If the expression of alpha-catenin is suppressed in the 5q- genotype or for other reasons, beta-catenin may be abnormally located or activated. In this study, abnormalities of chromosome 5 were associated with the presence of NPBC but this was not statistically significant. The reason why NPBC is associated with chromosome 7 abnormalities remains unclear. A gene encoded by chromosome 7 may be associated with the regulation of the Wnt/beta-catenin pathway. Several possible candidate genes including *SFRP4*, *WNT2*, and *FZD1* and *FZD9* are located at human chromosome 7. There are reports that sFRP4 plays a role in tumor suppression via the Wnt pathway (Hrzenjak *et al*, 2004; Horvath *et al*, 2007), although the specific relationship remains unknown. Since many molecules are directly or indirectly associated with the phosphorylation, stabilization and nuclear translocation of beta-catenin, the presence of nuclear NPBC might provide a clue to find a new leukemia-associated signaling mechanism.

In conclusion, *in situ* detection of nuclear NPBC by immunohistochemistry of paraffin sections from BM specimens could be used to predict the prognosis of AML and MDS. Understanding the mechanisms leading to leukemogenesis in nuclear NPBC$^+$ AML and MDS may lead to new anti-leukemia therapies.

Acknowledgements

This study is partly supported by Grants-in-Aid from National Institute of Biomedical Innovation and from Ministry of Education, Culture, Sports, Science and Technology on the Scientific Research. We thank Kazuko Matsuba for technical assistance, and Mari Otsuka for secretarial assistance.

References

Austin, T.W., Solar, G.P., Ziegler, F.C., Liem, L. & Matthews, W. (1997) A role for the Wnt gene family in hematopoiesis: expansion of multilineage progenitor cells. *Blood*, **89**, 3624–3635.

Bafico, A., Liu, G., Goldin, L., Harris, V. & Aaronson, S.A. (2004) An autocrine mechanism for constitutive Wnt pathway activation in human cancer cells. *Cancer Cell*, **6**, 497–506.

Barker, N. & Clevers, H. (2000) Catenins, wnt signaling and cancer. *BioEssays*, **22**, 961–965.

Bienz, M. & Clevers, H. (2000) Linking colorectal cancer to Wnt signaling. *Cell*, **103**, 311–320.

Chung, E.J., Hwang, S.G., Nguyen, P.M., Lee, S., Kim, J.S., Kim, J.W., Henkart, P.A., Bottaro, D.P., Soon, L.L., Bonvini, P., Lee, S.J., Karp, J.E., Oh, H.J., Rubin, J.S. & Trepel, J.B. (2002) Regulation of leukemic cell adhesion, proliferation and survival by beta-catenin. *Blood*, **100**, 982–990.

Cobas, M., Wilson, A., Ernst, B., Mancini, S.J.C., MacDonald, H.R., Kemler, R. & Radtke, F. (2004) Catenin is dispensable for hematopoiesis and lymphopoiesis. *Journal of Experimental Medicine*, **199**, 221–229.

Conacci-Sorrell, M., Zhurinsky, J. & Ben-ZeÂfev, A. (2002) The cadherin-catenin adhesion system in signaling and cancer. *Journal of Clinical Investigation*, **109**, 987–991.

Derksen, P.W.B., Tjin, E., Meijer, H.P., Klok, M.D., Mac Gillavry, H.D., Oers, M.H.J.V., Lokhorst, H.M., Bloem, A.C., Clevers, H., Nusse, R., Neut, R.V.D., Spaargaren, M. & Pals, S.T. (2004) Illegitimate WNT signaling promotes proliferation of multiple myeloma cells. *Proceedings of the National Academy of Sciences of the United States of America*, **101**, 6122–6127.

Etheridge, S.L., Spencer, G.J., Heath, D.J. & Genever, P.G. (2004) Expression profiling and functional analysis of wnt signaling mechanisms in mesenchymal stem cells. *Stem Cells*, **22**, 849–860.

Giles, R.H., van Es, J.H. & Clevers, H. (2003) Caught up in a Wnt storm: Wnt signaling in cancer. *Biochimica et Biophysica Acta*, **1653**, 1–24.

He, T.C., Sparks, A.B., Rago, C., Hermeking, H., Zawel, L., da Costa, L.T., Morin, P.J., Vogelstein, B. & Kinzler, K.W. (1998) Identification of c-MYC as a target of the APC pathway. *Science*, **281**, 1509–1512.

Heaney, M.L. & Golde, D.W. (1999) Articles medical progress: myelodysplasia. *New England Journal of Medicine*, **340**, 1649–1660.

Hirai, H. (2003) Molecular mechanisms of myelodysplastic syndrome. *Japanese Journal of Clinical Oncology*, **33**, 153–160.

Horvath, L.G., Lelliott, J.E., Kench, J.G., Lee, C.S., Williams, E.D., Saunders, D.N., Grygiel, J.J., Sutherland, R.L. & Henshall, S.M. (2007) Secreted frizzled-related protein 4 inhibits proliferation and metastatic potential in prostate cancer. *Prostate*, **67**, 1081–1090.

Hrzenjak, A., Tippl, M., Kremser, M.L., Strohmeier, B., Guelly, C., Neumeister, D., Lax, S., Moinfar, F., Tabrizi, A.D., Isadi-Moud, N., Zatloukal, K. & Denk, H. (2004) Inverse correlation of secreted frizzled-related protein 4 and -catenin expression in endometrial stromal sarcomas. *The Journal of Pathology*, **204**, 19–27.

Jamieson, C.H.M., Ailles, L.E., Dylla, S.J., Muijtjens, M., Jones, C., Zehnder, J.L., Gotlib, J., Li, K., Manz, M.G., Keating, A., Sawyers, C.L. & Weissman, I.L. (2004) Granulocyte-macrophage progenitors as candidate leukemic stem cells in blast-crisis CML. *New England Journal of Medicine*, **351**, 657–667.

Liu, T.X., Becker, M.W., Jelinek, J., Wu, W.S., Deng, M., Mikhalkevich, N., Hsu, K., Bloomfield, C.D., Stone, R.M., DeAngelo, D.J., Galinsky, I.A., Issa, J.P., Clarke, M.F. & Look, A.T. (2006) Chromosome 5q deletion and epigenetic suppression of the gene encoding -catenin (CTNNA1) in myeloid cell transformation. *Nature Medicine*, **13**, 78–83.

Morin, P.J., Sparks, A.B., Korinek, V., Barker, N., Clevers, H., Vogelstein, B. & Kinzler, W.K. (1997) Activation of beta-catenin-Tcf signaling in colon cancer by mutations in beta-catenin or APC. *Science*, **275**, 1787–1790.

Noort, M.V., Meeldijk, J., Zee, R.V.D., Destree, O. & Clevers, H. (2002) Wnt signaling controls the phosphorylation status of beta-catenin. *Journal of Biological Chemistry*, **277**, 17901–17905.

Ozeki, K., Kiyoi, H., Hirose, Y., Iwai, M., Ninomiya, M., Kodera, Y., Miyawaki, S., Kuriyama, K., Shimazaki, C., Akiyama, H., Nishimura, M., Motoji, T., Shinagawa, K., Takeshita, A., Ueda, R., Ohno, R., Emi, N. & Naoe, T. (2004) Biologic and clinical significance of the FLT3 transcript level in acute myeloid leukemia. *Blood*, **103**, 1901–1908.

Polakis, P. (2000) Wnt signaling and cancer. *Genes and Development*, **14**, 1837–1851.

Reya, T., Duncan, A.W., Ailles, L., Dome, J., Scherer, D.C., Willert, K., Hintz, L., Nusse, R. & Weissman, I.L. (2003) A role for Wnt signaling in self-renewal of hematopoietic stem cells. *Nature*, **423**, 409–414.

Serinsöz, E., Neusch, M., Büsche, G., Wasielewski, R.V., Kreipe, H. & Bock, O. (2004) Aberrant expression of beta-catenin discriminates acute myeloid leukaemia from acute lymphoblastic leukaemia. *British Journal of Haematology*, **126**, 313–319.

Simon, M., Grandage, V.L., Linch, D.C. & Khwaja, A. (2005) Constitutive activation of the Wnt/beta-catenin signalling pathway in acute myeloid leukaemia. *Oncogene*, **24**, 2410–2420.

Staal, F.J.T., Noort, M.V., Strous, G.J. & Clevers, H.C. (2002) Wnt signals are transmitted through N-terminally dephosphorylated beta-catenin. *EMBO Reports*, **3**, 63–68.

Tetsu, O. & Maccormick, F. (1999) Catenin regulates expression of cyclin D1 in colon carcinoma cells. *Nature*, **398**, 422–426.

Tickenbrock, L., Schwable, J., Wiedehage, M., Steffen, B., Sargin, B., Choudhary, C., Brandts, C., Berdel, W.E., Tidow, C.M. & Serve, H. (2005) Flt3 tandem duplication mutations cooperate with Wnt signaling in leukemic signal transduction. *Blood*, **105**, 3699–3706.

Van Den Berg, D.J., Sharma, A.K., Bruno, E. & Hoffman, R. (1998) Role of members of the Wnt gene family in human hematopoiesis. *Blood*, **92**, 3189–3202.

Willert, K., Brown, J.D., Danenberg, E., Duncan, A.W., Weissman, I.L., Reya, T., Yates, J.R. & Nusse, R. (2003) Wnt proteins are lipid-modified and can actas stem cell growth factors. *Nature*, **423**, 448–452.

Xu, J.L., Lai, R., Kinoshita, T., Nakashima, N. & Nagasaka, T. (2002) Proliferation, apoptosis and intratumoral vascularity in multiple myeloma: correlation with the clinical stage and cytologic grade. *Journal of Clinical Pathology*, **55**, 530–534.

Ysebaert, L., Chicanne, G., Demur, C., Toni, F.D., Houdellier, N.P., Ruidavets, J.B., Mas, V.M.D., Huguet, F.R., Laurent, G., Payrastre, B., Manenti, S. & Sultan, C.R. (2006) Expression of beta-catenin by acute myeloid leukemia cells predicts enhanced clonogenic capacities and poor prognosis. *Leukemia*, **20**, 1211–1216.

Pathology International 2007; **57**: 645–651 doi:10.1111/j.1440-1827.2007.02153.x

Original Article

Wilms' tumor 1 message and protein expression in bone marrow failure syndrome and acute leukemia

Takashi Iwasaki,[1,2] Chiho Sugisaki,[2,3] Kohzo Nagata,[2] Kenji Takagi,[2] Akira Takagi,[2] Tetsuhito Kojima,[2] Masafumi Ito,[4] Shigeo Nakamura,[1] Tomoki Naoe[5] and Takashi Murate[2]

[1]Department of Laboratory Medicine, Nagoya University School of Medicine, [2]Nagoya University School of Health Sciences, [3]Mitsubishi Nagoya Hospital, [4]Department of Pathology, Japanese Red Cross, Nagoya First Hospital, and [5]Department of Hematology and Oncology, Nagoya University School of Medicine, Nagoya, Japan

Wilms' tumor 1 (WT1) is a useful marker for the diagnosis of acute leukemia and myelodysplastic syndromes (MDS). In the current study quantitative reverse transcription–polymerase chain reaction and immunostaining were used simultaneously to examine the relationship between *WT1* RNA and protein level and also to evaluate WT1 as a tool to differentiate aplastic anemia (AA) and MDS refractory anemia (RA). Three types of *WT1* messages (total, exon 5(+) and KTS(+)) and WT1 immunostaining of these diseases were analyzed. An increase of all three *WT1* messages in high-grade MDS and acute leukemia was observed as compared with the normal control, whereas there was no significant difference in *WT1* message between AA and RA, suggesting that *WT1* message is not a good tool to discriminate AA and RA. No significant difference was observed between normal and RA, except for exon 5 message. Three *WT1* message levels had a significant correlation, suggesting that the total WT1 message is sufficient for clinical practice. Positive immunostaining of WT1 was observed only in the portion of acute leukemia and overt leukemia (OL) transformed from MDS with a high *WT1* message level, suggesting the relatively high detection threshold of WT1 protein with the immunostaining method.

Key words: acute leukemia, aplastic anemia, exon 5, immunostaining, KTS, MDS, quantitative RT-PCR, WT1 message

Wilms' tumor gene (*WT1*) is a tumor suppressor gene coding for a zinc finger transcription factor located on chromosome 11p13, which was originally identified for its involvement in the pathogenesis of Wilm's tumor.[1] WT1 is expressed in a variety of normal tissues, including ovary, testis, and spleen, while WT1 expression is low in normal bone marrow.[1] On the contrary, the *WT1* message was increased in acute leukemia and myelodysplastic syndromes (MDS)[2–5] and was regarded as an oncogene in some situations. The usefulness of *WT1* message level quantification has been reported in the detection of minimal residual disease and the relapse of acute leukemia.[2,6,7]

MDS are acquired clonal hematopoietic stem cell disorders characterized by ineffective dysplastic hematopoiesis involving one of more cell lineages and characterized by peripheral-blood cytopenias and a high risk of progression to acute leukemia.[8] Recently, the term bone marrow failure syndromes (BFS) was used from the standpoint of stem cell disorder, and both MDS and aplastic anemia were included in this category. However, because of the difference in treatment strategy, the differential diagnosis of MDS, especially refractory anemia (RA) and aplastic anemia (AA), is crucial but sometimes difficult.

Cilloni *et al.* reported the statistical significance of *WT1* message between normal bone marrow and RA bone marrow.[9] Even in their study, however, considerable overlap was observed between the *WT1* message of RA and those of normal control. Patmasiriwat *et al.* reported no statistically significant difference in the *WT1* message level between RA and normal control,[10] and the *WT1* message was not compared between RA and AA. Because the differential diagnosis between RA and non-severe AA is especially difficult when chromosomal abnormality and morphological dysplasia are not present, a new clinical parameter is needed. The aim of the present study was to analyze the *WT1* message level in BFS and also to evaluate the significance of *WT1* message level for the differential diagnosis of RA and AA.

WT1 is known to have four major isoforms due to the alternative splicing,[11] and it is also of interest to know the significance of these isoforms in MDS pathogenesis as well as the relative importance of each isoform as a clinical marker.

Correspondence: Takashi Murate, MD, Nagoya University School of Health Sciences, Daiko Minami 1-1-20, Higashi-ku, Nagoya 461-8673, Japan. Email: murate@met.nagoya-u.ac.jp

Received 6 March 2007. Accepted for publication 27 May 2007.

The gene expression level of each *WT1* splice variant in MDS has not been reported to date. Thus, we sought to analyze the message level of total *WT1*, exon 5(+) *WT1* and KTS(+) *WT1* in BFS and de novo acute leukemia.

The comparison of WT1 protein and *WT1* message level in MDS and acute leukemia are clinically important to determine the usefulness of immunostaining for routine laboratory examination of these diseases. Hence, we performed WT1 immunostaining of the clot section in patients whose *WT1* message level was measured. Previous histochemical analysis showed that many solid tumors and cancer cell lines express increased WT1 protein, but it is located sometimes in the cytoplasm, not the nucleus.[12–14] This might suggest that the role of WT1 in such cases is not that of a transcription factor. It was also shown that the *WT1* mRNA expression level does not correlate with the WT1 protein expression level.[13] Therefore, the significance of enhanced WT1 expression in solid tumor as well as in hematological malignancies remains to be determined.

MATERIALS AND METHODS

Clinical samples

After obtaining informed consent, bone marrow cells were collected from seven patients with AA, 28 with de novo acute myelocytic leukemia (AML) and 38 with MDS (17 RA, 21 refractory anemia with excessive blast (RAEB) and RAEB in transformation (RAEB-T) according to French–American–British classification) along with seven patients having overt leukemia developed from the previous MDS stage (OL). We used RAEB and RAEB-T as a single category because of the limited number of RAEB cases. Samples were obtained before any treatment. For the normal control, bone marrow samples for the disease staging were used from 11 patients with non-Hodgkin's lymphoma without bone marrow invasion. The clinical characteristics of AML and MDS patients are given in Table 1.

Quantitative reverse transcription–polymerase chain reaction

Mononuclear cells were separated from the bone marrow samples. RNA was extracted, and first-strand cDNA was prepared as described previously.[15] The primer set and reaction condition were according to Siehl *et al.*[16] After preliminary confirmation of the validity of the measurement of total *WT1*, exon 5(+) and KTS(+) *WT1* messages but not of exon 5(−) and KTS(−) messages by their method, we examined total *WT1*, exon 5(+) *WT1* and KTS(+) *WT1* messages of the present patient cohort. Primers and Taqman probe are listed in Table 2. PCR amplification was 40 cycles with the denaturing temperature at 95°C for 10 s followed by 60°C for 15 s.

Table 1 Patient characteristics

FAB	No. patients	Sex M	Sex F	Age (mean) (years)	Chromosome abnormality *n* (%)
AA	7	2	5	42.9	0 (0)
RA	17	11	6	60.9	4 (23.5)
RAEB/RAEB-T	21	14	7	66.3	9 (42.9)
OL	7	3	4	68.7	6 (85.7)
AML	28	19	9	51.7	12 (42.9)

AA, aplastic anemia; AML, acute myelocytic leukemia; FAB, French–American–British; MDS-OL, overt leukemia transformed from myelodysplastic syndromes; RA, refractory anemia; RAEB/RAEB-T, refractory anemia with excessive blast/refractory anemia with excessive blast in transformation.

Table 2 Primer and TaqMan probe sequences for quantitative RT-PCR

Total WT-1	
Forward	5′-CGCTATTCGCAATCAGGGTTAC-3′
Reverse	5′-ATGGGATCCTCATGCTTGAATG-3′
TaqMan Probe	5′-FAM-CGGTCACCTTCGACGGGACGC-TAMRA-3′
EXON 5(+)	
Forward	5′-TGGACAGAAGGGCAGAGCA-3′
Reverse	5′-GGATGGGCGTTGTGTGGT-3′
TaqMan Probe	5′-FAM-CCACAGCACAGGGTACGAGAGCGA-TAMRA-3′
KTS(+)	
Forward	5′-GCTCAAAAGACACCAAAGGAGAC-3′
Reverse	5′-AGCTGAAGGGCTTTTCACTTGTTT-3′
TaqMan Probe	5′-FAM-TTCTCCCGGTCCGACCACCTGAA-TAMRA-3′

Sequences are shown according to Siehl *et al.*[16] for of each primer set and Taqman probe used in quantitative RT-PCR.
RT-PCR, reverse transcription–polymerase chain reaction.

Quantification of total-*WT1* and splice variants (exon 5(+) *WT1* and KTS(+) *WT1*) was performed with the Light Cycler system (Roche Diagnostics, Mannheim, Germany). The housekeeping gene *ABL* mRNA was also measured as the internal control according to the recommendation of Beillard *et al.*[17] The relative ratio (*WT1/ABL*) was calculated and presented. Briefly, 1 μL of each cDNA was diluted to a volume of 19 μL PCR mix (LightCycler TaqMan Master, Roche Diagnostics), containing 0.5 pmol of each primer and 0.2 pmol of the TaqMan probe. The standard curve of *WT1* was created using the cDNA fragment of each *WT1*, which was produced by PCR and inserted into the cloning vector, pBluescript (Stratagene, La Jolla, CA, USA). The standard curve of *ABL* plasmid was also prepared. The specificity of each PCR product was confirmed in the preliminary experiments using leukemia cell lines.

Immunostaining

Formalin-fixed, paraffin-embedded bone marrow tissues were used for the immunostaining. Antigen retrieval was performed by microwave in 10 mmol/L citrate buffer (pH 7.4). Sections were blocked with PBS containing 5% skim milk, and then were reacted with anti-WT1 monoclonal antibody (clone 6F-H2, Dakocytomation, Carpinteria, CA, USA) at 4°C overnight. Endogenous peroxidase activity was blocked with 0.3% H_2O_2 in methanol solution. The detection was performed using the ChemMate EnVision Detection Kit/HRP (DAB) (Dakocytomation). The grading of WT1-positive cells was as follows: positive (+), >5% of total nuclei; weakly positive (+/–), 1–5% of total nuclei.

Statistical analysis

Results of clinical samples were analyzed using Microsoft Excel and Statview version 5 (SAS Institute, Cary, NC, USA). The statistical significance of differences between each group was assessed by one-way factorial analysis of variance and multiple comparison tests (Fisher's method). $P < 0.05$ was regarded as statistically significant.

RESULTS

Total *WT1* message level in AA, MDS, MDS-OL and AML

According to Table 1 the mean age of AA and AML patients is slightly lower than those of other groups, chromosome abnormality was absent in AA, and was increased with the progression of MDS stage (from RA to RAEB/RAEB-T). Figure 1 illustrates the distribution of total *WT1* message in normal, AA, MDS, OL and AML. In MDS bone marrow a statistically significant difference was observed between RA and RAEB/RAEB-T. OL and AML had a much higher expression level than RA but no statistically significant differences were observed between normal and AA, between normal and RA or between AA and RA, respectively.

WT1 immunostaining of bone marrow clot section

Nuclear staining was evident using our staining method (Fig. 1). Positive WT1 staining in each disease category was also shown in red (+) or blue (+/–) on the left side of Fig. 1. Strong positive staining was observed only in AML (8/28 cases, 28.6%) and OL (1/7 cases, 14.3%). In MDS, weakly positive (+/–) staining but not strong positive staining was observed in some cases (4/21 RAEB/RAEB-T, 19%; 4/17 RA, 23.5%). No positive staining was observed in AA or normal groups. The staining intensity of each positive cell was apparently higher in AML and OL than in MDS. When combined with *WT1* message and immunostaining data, the positive staining clearly required the high *WT1* message expression in whole bone marrow (Fig. 1). The threshold is approximately 1/10 of the *ABL* message level. Normal bone marrow contained approximately 10^5 copies of *ABL*/μg RNA according to previous reports[17,18] and our preliminary experiments. Therefore, the threshold for positive WT1 staining was 10^4 copies/μg RNA of total bone marrow. In other words, a value exceeding this threshold can indeed confirm the presence of leukemic bone marrow. It is interesting to examine the CD34 population of MDS bone marrow because the present data suggest that the *WT1* message might be proportional to the blast cell percentage in MDS. But we could not examine this point in the present study because of the paucity of samples. It is of note that the *WT1* message level in AML and OL is heterogeneous, suggesting that the WT1 staining pattern of bone marrow is not always proportional to the percentage of blast cells. It can be said that the sensitivity of WT1 staining is relatively low as compared with reverse transcription–polymerase chain reaction (RT-PCR).

Exon 5 and KTS+ *WT1* message level in BFS and AML

The message level of exon 5(+) and KTS(+) *WT1* is shown in Fig. 2. Statistically significant differences were also observed in exon 5 *WT1* message between RA and RAEB/RAEB-t (Fig. 2). Only in this isoform was a statistically significant difference observed between normal and MDS RA; no similar tendency was observed between normal and AA, or between AA and RA. Analysis of KTS(+) *WT1* message found a similar tendency (Fig. 2), that is, an increase of message during the progression of MDS and the lack of significant differences between normal and AA, normal and RA, or AA and RA, respectively.

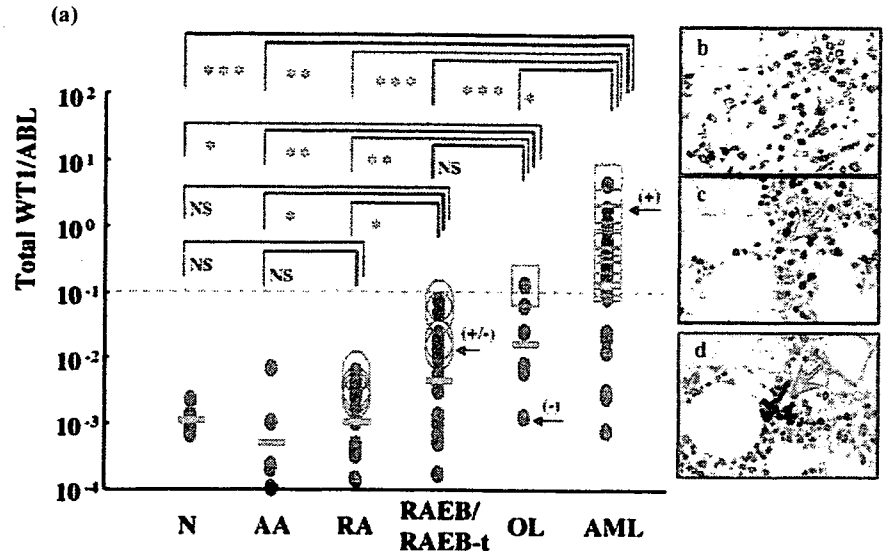

Figure 1 (**a**) Total Wilms' tumor 1 (*WT1*) message level was examined using quantitative (TaqMan) reverse transcription–polymerase chain reaction (RT-PCR). The y axis indicates the ratio of total *WT1/ABL* message (relative *WT1* message level) shown as the log scale. N, normal; AA, aplastic anemia; RA, refractory anemia; RAEB/RAEB-T, refractory anemia with excessive blast/refractory anemia with excessive blast in transformation; OL, overt leukemia transformed from myelodysplastic syndrome; AML, acute myelocytic leukemia. Horizontal bar, mean; broken line, putative threshold for WT1-positive immunostaining; red squares, WT1-positive staining; blue circles, weakly positive staining according to the criteria described in the present study. (**b–d**) Representative staining patterns of WT1. Arrow indicates nuclear staining positive cells. (**b**) Negative staining was from OL (a, black arrow); (**c**) weakly positive staining (+/–) was from RAEB/RAEB-T (a, black arrow); (**d**) strong positive staining (+) was from AML (a, black arrow). NS, not significant. $^{*}P < 0.05$, $^{**}P < 0.001$, $^{***}P < 0.0001$ according to one-way factorial analysis of variance and multiple comparison test (Fisher's method).

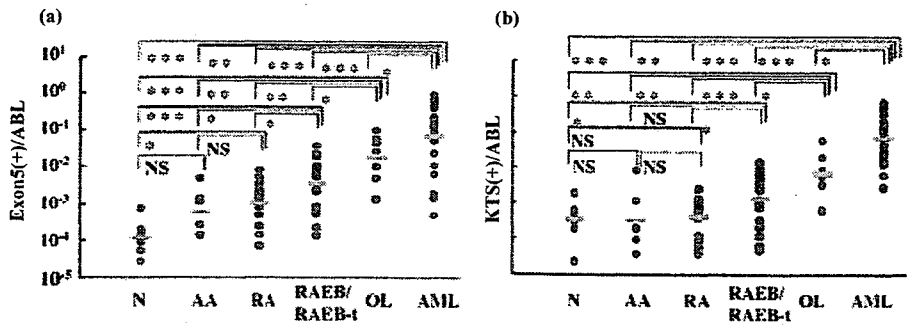

Figure 2 (**a**) Exon 5(+) and (**b**) KTS(+) Wilms' tumor 1 (*WT1*) message analyzed on quantitative reverse transcription–polymerase chain reaction (RT-PCR). Data are expressed as the ratio of the message of each *WT1* isoform/*ABL*. Specific primer sets are as described in Table 2. N, normal; AA, aplastic anemia; RA, refractory anemia; RAEB/RAEB-T, refractory anemia with excessive blast/refractory anemia with excessive blast in transformation; OL, overt leukemia transformed from myelodysplastic syndrome; AML, acute myelocytic leukemia. Horizontal bar, mean. NS, not significant. $^{*}P < 0.05$, $^{**}P < 0.001$, $^{***}P < 0.0001$ according to one-way factorial analysis of variance and multiple comparison test (Fisher's method).

Correlation between total *WT1* and exon 5(+) or between total *WT1* and KTS(+) message

Figure 3 shows a correlation between total *WT1* and exon 5(+) *WT1* and also between the total *WT1* and KTS(+) *WT1* message. Both graphs indicated a good correlation between these two indexes (total and each spliced form), denying the possibility that there is some unique distribution of special splice variant *WT1* message in the diseases analyzed. The results also suggest that the total *WT1* message analysis is sufficient for the clinical diagnosis and treatment of BFS and AML.

DISCUSSION

Because the mutations of the *WT1* gene were the cause of Wilms' tumor, Denys–Drash syndrome and Frasier syndrome, wild-type *WT1* has been regarded as the tumor suppressor gene.[11] After the discovery of WT1 overexpression in

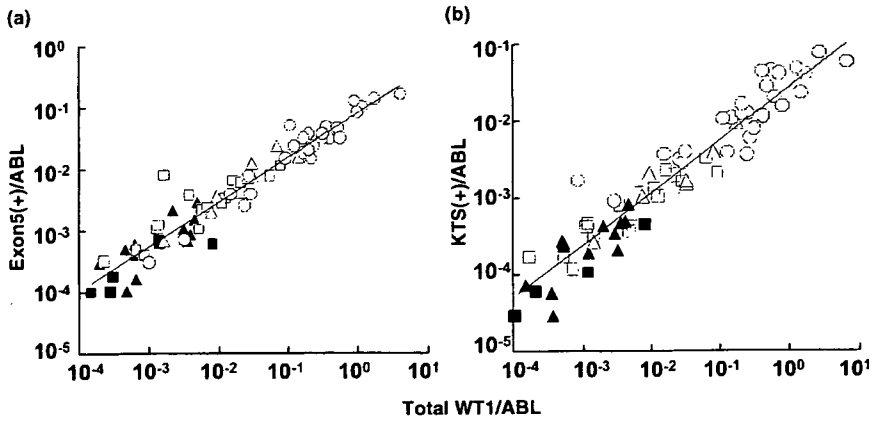

Figure 3 Correlation between total Wilms' tumor 1 (WT1) and (**a**) exon 5(+) *WT1* message and between total *WT1* and (**b**) KTS(+) *WT1* message in MDS, OL and AML, based on data of total *WT1*, exon 5(+) and KTS(+) *WT1* message level. (■) AA, aplastic anemia; (▲) RA, refractory anemia; (□) RAEB/RAEB-T, refractory anemia with excessive blast/refractory anemia with excessive blast in transformation; (△) OL, overt leukemia transformed from myelodysplastic syndrome; (○) AML, acute myelocytic leukemia. Correlation efficiency: a, $R^2 = 0.922$; b, $R^2 = 0.914$.

hematological malignancies,[3,4] WT1 was also taken to be the oncogene in some situations.[19] Importantly, Hosoya *et al.* reported the absence of mutation of *WT1* gene in MDS.[20] WT1 is a zinc finger protein and works as the transcription factor to regulate its target gene expression, but the respective function of four WT1 isoforms as the transcription factor has not been completely clarified. Therefore, the significance of each WT 1 isoform in malignant diseases also remains to be determined.

Siehl *et al.* reported that major splice variants could be separately calculated using their RT-PCR strategy.[16] A similar method was also reported using semiquantitative RT-PCR.[21] However, contrary to a previous report,[16] our preliminary analysis found that the combination of total *WT1*, exon 5(+), and KTS(+) *WT1* messages cannot always estimate exon 5(−) and KTS(−) *WT1* messages. Another method is necessary such as the RNase protection assay as reported by Haber *et al.*,[22] which needs a considerable amount of RNA in order to be performed. Therefore we presented and discussed the data of total *WT1*, exon 5(+) *WT1* and KTS(+) message of BFS and AML in the present study.

The relationship between total *WT1* message and International Prognostic Score System (IPSS) of MDS has been reported.[9] The *WT1* message level is considered to be a universal marker for minimal residual disease and quantification of leukemic cells.[23] It was also reported that *WT1* is highly expressed in the CD34(+) population of AML,[24] although some controversy remains as to whether or not the percentage of CD34 expression is related to the *WT1* message level.[25] The prognostic relevance of high *WT1* levels at diagnosis in acute leukemia is controversial.[26–29] Because the gradual increase of total *WT1* message was observed from low-grade MDS to AML, the present analysis is consistent with previous reports suggesting a good correlation between *WT1* message and MDS disease progression to overt leukemia.

Another important issue is the differential diagnosis between RA and non-severe AA when they have no morphological and/or chromosomal abnormality. We observed that total *WT1* as well as any isoform *WT1* messages could not clearly discriminate between normal and RA and between RA and AA, respectively. There was always some overlap of *WT1* message among normal, AA and RA. An expression level $>2 \times 10^{-3}$ *WT1/ABL* (higher than normal) might be regarded mostly as either MDS or AML. Although severe AA patients were excluded from the current analysis (mostly because of low RNA yield), the present results suggest the limitation of *WT1* message analysis in discriminating RA and AA. Several reports comparing the *WT1* level between RA and normal subjects have presented conflicting results.[9,10] Another possible interpretation of the present results is that *WT1* overexpression is not the early cellular event of RA.

Nakatsuka *et al.*[14] reported on *WT1* message level in various solid tumor cell lines, and >80% of them expressed the *WT1* message. These results were presumed to reflect the possible role of WT1 in the oncogenic process of solid tumors. But it was reported that there was no relationship between *WT1* message level and positive immunostaining.[12] Moreover, the problem in WT1 immunostaining of these solid tumors was the localization of WT1 protein in the cytoplasm but not in the nucleus. The present analysis showed clearly its nuclear localization in the bone marrow clot sections of MDS and AML. Cells staining positive for WT1 could be regarded as blast cells or leukemia cells.

The present study demonstrated positive staining only in AML and OL or in samples with $>10^4$ *WT1* copies/μg RNA. The present results suggest a difference in the sensitivity of each assay method (quantitative RT-PCR and immunostaining) for the quantification of *WT1* expression, and that the WT1 staining was not sufficiently sensitive for clinical practice in MDS and AML cases.

Numerous studies have confirmed that the specific effect of WT1 on cell death is critically dependent on the cell type being studied and that different WT1 isoforms can have a distinct effect on gene regulation and cell fate.[30,31] It is of interest to know whether some isoform of WT1 is particularly

important for leukemogenesis or which form of *WT1* is prevalent in hematological malignancy. Previous reports showed that exon 5(+) isoform was the dominant form in AML as well as lung, head and neck squamous carcinomas.[16,21] The present analysis suggested that both exon 5(+) and KTS(+) message was strongly correlated with the total *WT1* message level. It is less likely that other isoforms (exon 5 (–) or KTS (–)) played some unique role in the leukemogenesis. Recently, the anti-apoptotic function of the exon 5(+) *WT1* gene has also been reported.[32]

Taken together, the present analysis indicates a considerable overlap of *WT1* message among normal, AA and RA, and that WT1-positive nuclear immunostaining was clearly observed in patients whose *WT1* message of the bone marrow was higher than 1/10 the *ABL* gene message (or 10^4 copies/μg RNA). These data provide a basic understanding of WT1 expression in BFS and AML.

ACKNOWLEDGMENT

The authors express sincere thanks to Dr M. Suzuki (Nagoya University Graduate School of Medicine) for his valuable assistance in figure preparation.

REFERENCES

1 Reddy JC, Licht JD. The WT1 Wilms' tumor suppressor gene: How much do we really know? *Biochim Biophys Acta* 1996; **1287**: 1–28.
2 Inoue K, Sugiyama H, Ogawa H *et al.* WT1 as a new prognostic factor and a new marker for the detection of minimal residual disease in acute leukemia. *Blood* 1994; **84**: 3071–9.
3 Inoue K, Ogawa H, Sonoda Y *et al.* Aberrant overexpression of the Wilms tumor gene (WT1) in human leukemia. *Blood* 1997; **89**: 1405–12.
4 Tamaki H, Ogawa H, Inoue K *et al.* Increased expression of the Wilms tumor gene (WT1) at relapse in acute leukemia. *Blood* 1996; **88**: 4396–498.
5 Boublikova L, Kalinova M, Ryan J *et al.* Wilms' tumor gene 1 (WT1) expression in childhood acute lymphoblastic leukemia: A wide range of WT1 expression levels, its impact on prognosis and minimal residual disease monitoring. *Leukemia* 2006; **20**: 254–63.
6 Inoue K, Ogawa H, Yamagami T *et al.* Long-term follow-up of minimal residual disease in leukemia patients by monitoring WT1 (Wilms tumor gene) expression levels. *Blood* 1996; **88**: 2267–78.
7 Bader P, Niemeyer C, Weber G *et al.* WT1 gene expression: Useful marker for minimal residual disease in childhood myelodysplastic syndromes and juvenile myelo-monocytic leukemia. *Eur J Haematol* 2004; **73**: 25–8.
8 Phelan JT, Koides PA, Bennet JM. Myelodysplastic syndromes: Historical aspects. In: Bennet JM, ed. *The Myelodysplastic Syndromes*. New York: Marcel Dekker, 2002; 1–15.
9 Cilloni D, Gottardi E, Messa F *et al.* Significant correlation between the degree of WT1 expression and the International Prognostic Scoring System Score in patients with myelodysplastic syndromes. *J Clin Oncol* 2003; **21**: 1988–95.
10 Patmasiriwat P, Fraizer G, Kantarjian H, Saunders GF. WT1 and GATA1 expression in myelodysplastic syndrome and acute leukemia. *Leukemia* 1999; **13**: 891–900.
11 Hohenstein P, Hastie ND. The many facets of the Wilms' tumour gene, WT1. *Hum Mol Genet* 2006; **15**: 196–201.
12 Oji Y, Ogawa H, Tamaki H *et al.* Expression of the Wilms' tumor gene WT1 in solid tumors and its involvement in tumor cell growth. *Jpn J Cancer Res* 1999; **90**: 194–204.
13 Oji Y, Suzuki T, Nakano Y *et al.* Overexpression of the Wilms' tumor gene WT1 in primary astrocytic tumors. *Cancer Sci* 2004; **95**: 822–7.
14 Nakatsuka S, Oji Y, Horiuchi T *et al.* Immunohistochemical detection of WT1 protein in a variety of cancer cells. *Mod Pathol* 2006; **19**: 804–14.
15 Sobue S, Iwasaki T, Sugisaki C *et al.* Quantitative RT-PCR analysis of sphingolipid metabolic enzymes in acute leukemia and myelodysplastic syndromes. *Leukemia* 2006; **20**: 2042–6.
16 Siehl JM, Reinwald M, Heufelder K, Menssen HD, Keilholz U, Thiel E. Expression of Wilms' tumor gene 1 at different stages of acute myeloid leukemia and analysis of its major splice variants. *Ann Hematol* 2004; **83**: 745–50.
17 Beillard E, Pallisgaard N, van der Velden VH *et al.* Evaluation of candidate control genes for diagnosis and residual disease detection in leukemic patients using 'real-time' quantitative reverse-transcriptase polymerase chain reaction (RQ-PCR): An Europe against cancer program. *Leukemia* 2003; **17**: 2474–86.
18 Garg M, Moore H, Tobal K, John A, Liu Yin JA. Prognostic significance of quantitative analysis of WT1 gene transcripts by competitive reverse transcription polymerase chain reaction in acute leukaemia. *Br J Haematol* 2003; **123**: 49–59.
19 Loeb DM, Sukumar S. The role of WT1 in oncogenesis: Tumor suppressor or oncogene? *Int J Hematol* 2002; **76**: 117–26.
20 Hosoya N, Miyagawa K, Mitani K, Yazaki Y, Hirai H. Mutation analysis of the WT1 gene in myelodysplastic syndromes. *Jpn J Cancer Res* 1998; **89**: 821–4.
21 Oji Y, Miyoshi S, Maeda H *et al.* Overexpression of the Wilms' tumor gene WT1 in de novo lung cancers. *Int J Cancer* 2002; **100**: 297–302.
22 Haber DA, Sohn RL, Buckler AJ *et al.* Alternative splicing and genomic structure of the Wilms tumor gene WT1. *Proc Natl Acad Sci USA* 1991; **88**: 9618–22.
23 Cilloni D, Saglio G. WT1 as a universal marker for minimal residual disease detection and quantification in myeloid leukemias and in myelodysplastic syndrome. *Acta Haematol* 2004; **112**: 79–84.
24 Hosen N, Sonoda Y, Oji Y *et al.* Very low frequencies of human normal CD34+ haematopoietic progenitor cells express the Wilms' tumour gene WT1 at levels similar to those in leukaemia cells. *Br J Haematol* 2002; **116**: 409–20.
25 Weisser M, Kern W, Rauhut S *et al.* Prognostic impact of RT-PCR-based quantification of WT1 gene expression during MRD monitoring of acute myeloid leukemia. *Leukemia* 2005; **19**: 1416–23.
26 Trka J, Kalinov M, Hrusak O *et al.* Real-time quantitative PCR detection of WT1 gene expression in children with AML: Prognostic significance, correlation with disease status and residual disease detection by flow cytometry. *Leukemia* 2002; **16**: 1381–9.
27 Ostergaard M, Olesen LH, Hasle H, Kjeldsen E, Hokland P. WT1 gene expression: An excellent tool for monitoring minimal residual disease in 70% of acute myeloid leukaemia patients: Results from a single-centre study. *Br J Haematol* 2004; **125**: 590–600.
28 Gaiger A, Schmid D, Heinze G *et al.* Detection of the WT1 transcript by RT-PCR in complete remission has no prognostic

relevance in de novo acute myeloid leukemia. *Leukemia* 1998; **12**: 1886–94.
29 Schmid D, Heinze G, Linnerth B *et al.* Prognostic significance of WT1 gene expression at diagnosis in adult de novo acute myeloid leukemia. *Leukemia* 1997; **11**: 639–43.
30 Loeb DM. WT1 influences apoptosis through transcriptional regulation of Bcl-2 family members. *Cell Cycle* 2006; **5**: 1249–53.
31 Jomgeow T, Oji Y, Tsuji N *et al.* Wilms' tumor gene WT1 17AA(–)/KTS(–) isoform induces morphological changes and promotes cell migration and invasion in vitro. *Cancer Sci* 2006; **97**: 259–70.
32 Ito K, Oji Y, Tatsumi N *et al.* Antiapoptotic function of 17AA(+)WT1 (Wilms' tumor gene) isoforms on the intrinsic apoptosis pathway. *Oncogene* 2006; **25**: 4217–29.

Leukemia (2007) 21, 2476–2484

www.nature.com/leu

ORIGINAL ARTICLE

FLT3 regulates β-catenin tyrosine phosphorylation, nuclear localization, and transcriptional activity in acute myeloid leukemia cells

T Kajiguchi[1,4], EJ Chung[2], S Lee[2], A Stine[3], H Kiyoi[4], T Naoe[5], MJ Levis[3], L Neckers[1] and JB Trepel[2]

[1]Urologic Oncology Branch, National Cancer Institute, National Institutes of Health, Bethesda, MD, USA; [2]Medical Oncology Branch, National Cancer Institute, National Institutes of Health, Bethesda, MD, USA; [3]Sidney Kimmel Comprehensive Cancer Center at Johns Hopkins, Baltimore, MD, USA; [4]Department of Infectious Disease, Nagoya University Graduate School of Medicine, Nagoya, Japan and [5]Department of Hematology Oncology, Nagoya University Graduate School of Medicine, Nagoya, Japan

Deregulated accumulation of nuclear β-catenin enhances transcription of β-catenin target genes and promotes malignant transformation. Recently, acute myeloid leukemia (AML) cells with activating mutations of FMS-like tyrosine kinase-3 (FLT3) were reported to display elevated β-catenin-dependent nuclear signaling. Tyrosine phosphorylation of β-catenin has been shown to promote its nuclear localization. Here, we examined the causal relationship between FLT3 activity and β-catenin nuclear localization. Compared to cells with wild-type FLT3 (FLT3-WT), cells with the FLT3 internal tandem duplication (FLT3-ITD) and tyrosine kinase domain mutation (FLT3-TKD) had elevated levels of tyrosine-phosphorylated β-catenin. Although β-catenin was localized mainly in the cytoplasm in FLT3-WT cells, it was primarily nuclear in FLT3-ITD cells. Treatment with FLT3 kinase inhibitors or FLT3 silencing with RNAi decreased β-catenin tyrosine phosphorylation and nuclear localization. Conversely, treatment of FLT3-WT cells with FLT3 ligand increased tyrosine phosphorylation and nuclear accumulation of β-catenin. Endogenous β-catenin co-immunoprecipitated with endogenous activated FLT3, and recombinant activated FLT3 directly phosphorylated recombinant β-catenin. Finally, FLT3 inhibitor decreased tyrosine phosphorylation of β-catenin in leukemia cells obtained from FLT3-ITD-positive AML patients. These data demonstrate that FLT3 activation induces β-catenin tyrosine phosphorylation and nuclear localization, and thus suggest a mechanism for the association of FLT3 activation and β-catenin oncogenic signaling in AML.
Leukemia (2007) 21, 2476–2484; doi:10.1038/sj.leu.2404923;
published online 13 September 2007
Keywords: FLT3 AML; β-catenin; tyrosine phosphorylation

Introduction

FLT3 is a member of the class III receptor tyrosine kinase family and plays an important role in regulating the proliferation, differentiation and survival of hematopoietic cells.[1,2] Binding of FLT3 ligand (FL) to FLT3 promotes receptor dimerization and activation of FLT3.[1] The activated receptor then activates the phosphotidylinositol 3–kinase (PI3K) and RAS signal-transduction cascades.[3,4] FLT3 mutations are the most frequent genetic lesion seen in acute myeloid leukemia (AML). Of patients with AML, 15–35% have an internal tandem duplication (ITD) of the juxtamembrane domain of FLT3 (FLT3-ITD)[5–8] and 5–10% have mutations in the tyrosine kinase domain (TKD) of FLT3 (FLT3-TKD).[9,10] Both types of FLT3 mutation result in ligand-independent activation of the receptor and activation of downstream signaling pathways.[11–13] The presence of FLT3-ITD is associated with leukocytosis and poor clinical outcome in both pediatric and adult patients with AML.[7,8,14,15]

β-catenin is a multifunctional protein that plays an important role in both cell – cell interactions[16,17] and transcriptional regulation.[18–20] In epithelial cells, β-catenin is localized at the inner surface of the plasma membrane, where it functions in conjunction with E-cadherin as part of the adherens junction, a specialized cytoskeletal complex that regulates cell–cell adhesion.[21] β-catenin is also the critical effector of the canonical Wnt signaling pathway, in which nuclear β-catenin coactivates transcription in association with LEF/TCF family members. In the absence of secreted Wnts, the modular protein axin provides a scaffold for the binding of glycogen synthase kinase-3β (GSK-3β), adenomatous polyposis coli (APC) protein and β-catenin. This facilitates serine/threonine phosphorylation in the N terminus of β-catenin by GSK-3β and subsequent degradation of β-catenin by a proteasome-dependent process.[22,23] Wnt stimulation leads to β-catenin stabilization, nuclear accumulation and interaction with T-cell factor/lymphoid enhancer factor (TCF/LEF) transcription factors to regulate genes important for proliferation and survival.[18,24–26]

Wnt/β-catenin has previously been implicated in the development of several hematologic malignancies.[27–31] Recently, it was reported that TCF-dependent transcriptional activity of FLT3-ITD cells is higher than in FLT3-WT cells, suggesting that aberrant β-catenin signaling may contribute to FLT3-ITD-related myeloid transformation.[32] However, the relationship between FLT3 activity and activation of β-catenin-dependent nuclear signaling has not been elucidated. While serine/threonine phosphorylation facilitates degradation of β-catenin in the proteasome, we and others have demonstrated that tyrosine phosphorylation facilitates β-catenin nuclear localization and enhances β-catenin-associated transcription.[25,33,34] Thus far, tyrosine phosphorylation of β-catenin and a potential role for FLT3 in this regulatory event have not been examined in AML. In this study, we have examined the effects of FLT3 mutation or activation on β-catenin tyrosine phosphorylation, subcellular localization and transcriptional activity.

Correspondence: Dr T Kajiguchi, Department of Infectious Disease, Nagoya University Graduate School of medicine, 65 Tsurumai-cho, Showa-ku, Nagoya 466-8560, Japan.
E-mail: tomokaji@med.nagoya-u.ac.jp
Received 10 May 2007; revised 7 July 2007; accepted 23 July 2007; published online 13 September 2007

Materials and methods

Antibodies and reagents

FLT3 inhibitor AG1296 was purchased from Calbiochem (San Diego, CA, USA). The FLT3 inhibitor PKC 412 and GSK3β

inhibitor SB415286 were purchased from LC Laboratories (Woburn, MA, USA). FLT3 siRNA, β-catenin siRNA and control siRNA were purchased from Dharmacon (Lafayette, CO, USA). Recombinant human FLT3 ligand (FL) and recombinant mouse IL-3 were purchased from R&D systems (Minneapolis, MN, USA). Fetal bovine serum (FBS) was purchased from Gibco-BRL (Gaithersburg, MD, USA). Anti-β-catenin monoclonal antibody was purchased from BD Biosciences (San Jose, CA, USA). Anti-FLT3-antibody was purchased from Santa Cruz Biotechnology (Santa Cruz, CA, USA). Anti-phosphotyrosine monoclonal antibody was purchased from Upstate (Charlottesville, VA, USA). Anti-phospho-β-catenin antibody (Ser33/37/Thr41), anti-phospho-GSK3 antibody (Ser21/9), anti-GSK3β antibody and anti-topoisomerase II antibody were purchased from Cell Signaling Technology (Danvers, MA, USA). Western blotting blocking reagent was purchased from Roche Applied Science (Indianapolis, IN, USA). GammaBind Plus Sepharose beads and horseradish peroxidase (HRP)-labeled goat anti-mouse and goat anti-rabbit antibodies were purchased from Amersham Biosciences (Uppsala, Sweden). BCA Protein Assay reagent, western blot chemiluminescence reagents and Restore Western Blot Stripping Buffer were purchased from Pierce Chemical Co (Rockford, IL, USA). PVDF membrane was purchased from Bio-Rad Laboratories (Hercules, CA, USA).

Cells

The murine IL-3-dependent myeloid progenitor cell line, 32D, was obtained from the RIKEN cell bank (Tsukuba, Japan) and maintained in RPMI-1640 medium supplemented with 10% fetal bovine serum and 1.0 ng ml^{-1} recombinant murine IL-3. WT, ITD and TKD (D835) FLT3-expressing 32D cell lines were reported previously.[10–12,35] MOLM-13, a human AML-M5 cell line with the FLT3-ITD mutation,[6] was kindly provided by Dr Yoshinobu Matsuo (Fujisaki Cell Center, Okayama, Japan). MV 4-11, a human AML cell line expressing FLT3-ITD, and THP-1, a human AML-M5 cell line expressing FLT3-WT,[6] were purchased from ATCC (Manassas, VA, USA). MOLM-13 and THP-1 were maintained in RPMI-1640 medium supplemented with 10% FBS. MV 4-11 was maintained in Iscove's modified Dulbecco's medium (IMDM) with 20% FBS.

Immunoprecipitation and immunoblotting assays. Cells were washed twice with ice-cold PBS, and were lysed in lysis buffer (20 mM Tris–HCl, pH 7.5, 150 mM NaCl, 2 mM EDTA, 1% Triton X-100, 50 mM NaF, 1 mM Na_3VO_4, 10 μg ml^{-1} aprotinin, 10 μg ml^{-1} leupeptin and 1 mM phenylmethylsulfonyl fluoride). After incubation for 1 h at 4 °C, lysates were spun at 12 000 *g* for 25 min and pellets were discarded. Lysates were immunoprecipitated with each primary antibody overnight at 4 °C. GammaBind Plus Sepharose (GE Healthcare Bio-Sciences Corp., Piscataway, NJ, USA) beads were added and the mixture was rocked for 1 h at 4 °C. The beads were subsequently washed three times with lysis buffer and mixed with sodium dodecyl sulfate (SDS) sample buffer. After boiling for 5 min, samples were separated by SDS-polyacrylamide gel electrophoresis (SDS-PAGE) and electroblotted onto PVDF membranes (Millipore, Billerica, MA, USA). The membranes were incubated overnight with primary antibody in 10% blocking reagent in TNE washing buffer: (50 mM NaCl, 10 mM Tris–HCl, pH 7.5, 2.5 mM EDTA, 0.1% Tween 20). Primary antibodies were detected by HRP-labeled secondary antibody (1:2000) and were visualized using chemiluminescence reagents. For reprobing, the membranes were stripped with stripping buffer and reprobed with the indicated antibodies. Band optical densities were measured using a GS-800 densitometer and Quantity One software (Bio-Rad).

Immunocytochemistry

Cells that had been attached to glass slides by cytocentrifugation (Shandon, Pittsburgh, PA, USA) were fixed with 3.7% formaldehyde in PBS for 10 min and permeabilized with 0.2% Triton X-100 for another 10 min at room temperature. The cells were stained with monoclonal anti-β-catenin antibody (BD Biosciences), Alexa Fluor 488 goat anti-mouse immunoglobulin (Molecular Probes, Carlsbad, CA, USA) and 4′,6-diamidino-2-phenylindole (DAPI; Molecular Probes). The cells were viewed using a Leica DM IRB fluorescence microscope (×100 objective) equipped with a *Z*-axis motor (Ludl Electronics, Hawthorne, NY, USA). Stacks of images (13–19 optical sections at a step size of 0.3 μm) were taken with a digital camera (Hamamatsu) and processed using Openlab Volume Deconvolution software (Improvision, Lexington, MA, USA). Nuclear β-catenin was determined using the colocalization feature in Openlab. Briefly, the areas of colocalization, depicted as violet, were generated by calculation of measurement statistics based on intensity information in the whole image obtained from two fluorescence channels detecting β-catenin and DAPI.

Preparation of subcellular fractions

Cells were washed and treated with ice-cold low-salt lysis buffer (10 mM HEPES, pH 7.9, 10 mM KCl, 1 mM Na_3VO_4, 10 μg ml^{-1} aprotinin, 10 μg ml^{-1} leupeptin) for 10 min at 4 °C. Cells were homogenized with 15 strokes of a Dounce homogenizer. Homogenates were centrifuged at 700 *g* for 5 min and supernatant fractions were saved as cytoplasmic extracts. The pellets were resuspended in high-salt lysis buffer (20 mM HEPES, pH 7.9, 25% glycerol, 420 mM NaCl, 1% TritonX-100, 1 mM Na_3VO_4, 10 μg ml^{-1} aprotinin, 10 μg ml^{-1} leupeptin) and rotated for 10 min at 4 °C. Cellular debris was removed by centrifugation and supernatants were saved as nuclear fractions. Equal amounts of protein were subjected to western blot analysis.

Quantitative Reverse Transcriptase-PCR. Total RNA was isolated using the RNeasy Mini Kit (Qiagen, Valencia, CA, USA) and cDNA was prepared using the TaqMan Reverse Transcription Kit (Applied Biosystems, Foster City, CA, USA). Analysis of mRNA expression was carried out by real-time RT-PCR using the ABI Prism 7700 Sequence Detection System (Applied Biosystems). All sample mRNA levels were normalized to the level of 18S ribosomal RNA. The primer and probe sequences for real-time RT-PCR were as follows: rRNA forward 5′-AGTCCCTGCC CTTTGTACACA-3′, rRNA reverse 5′-CGATCCGAGGGCCTC ACTA-3′, c-*myc* forward 5′-CGTCTCCACACATCAGCACAA-3′, c-*myc* reverse 5′-TCTTGGCAGCAGGATAGTCCTT-3′, cyclin D1 forward 5′-GCATGTTCGTGGCCTCTAAGAT-3′, cyclin D1 reverse 5′-TCGGTGTAGATGCACAGCTTCT-3′.

In vitro *kinase assay*

Recombinant β-catenin (Upstate) was incubated with or without recombinant FLT3 kinase (Cell Signaling Technology) in reaction buffer (60 mM HEPES pH 7.5, 5 mM $MgCl_2$, 5 mM $MnCl_2$, 3 μM Na_3VO_4, 1.25 mM DTT, 200 μM ATP) for 30 min at 25 °C. After the reaction, samples were mixed with SDS-sample buffer and were resolved by SDS-PAGE, electrotransferred and immunoblotted with anti-phospho-tyrosine antibody (Upstate). The membrane was stripped and reprobed with

anti-β-catenin antibody. Since albumin is not phosphorylated by FLT3, the membrane was stained with Ponceau S to identify the location of albumin.

RNAi-mediated silencing of FLT3

MOLM-13 cells (2×10^6 in 100 µl) were transfected with 1 µM FLT3 siRNA, β-catenin siRNA or control siRNA by electroporation (Nucleofector, Amaxa Biosystems, Gaithersburg, MD, USA). Following transfection, the cells were incubated for 48 h and then were subjected to immunoprecipitation and immunoblot assay. Band optical density was measured using a GS-800 densitometer and Quantity One software.

Primary AML samples

Bone marrow and peripheral blood samples were obtained from leukemia patients under an Institutional Review Board-approved

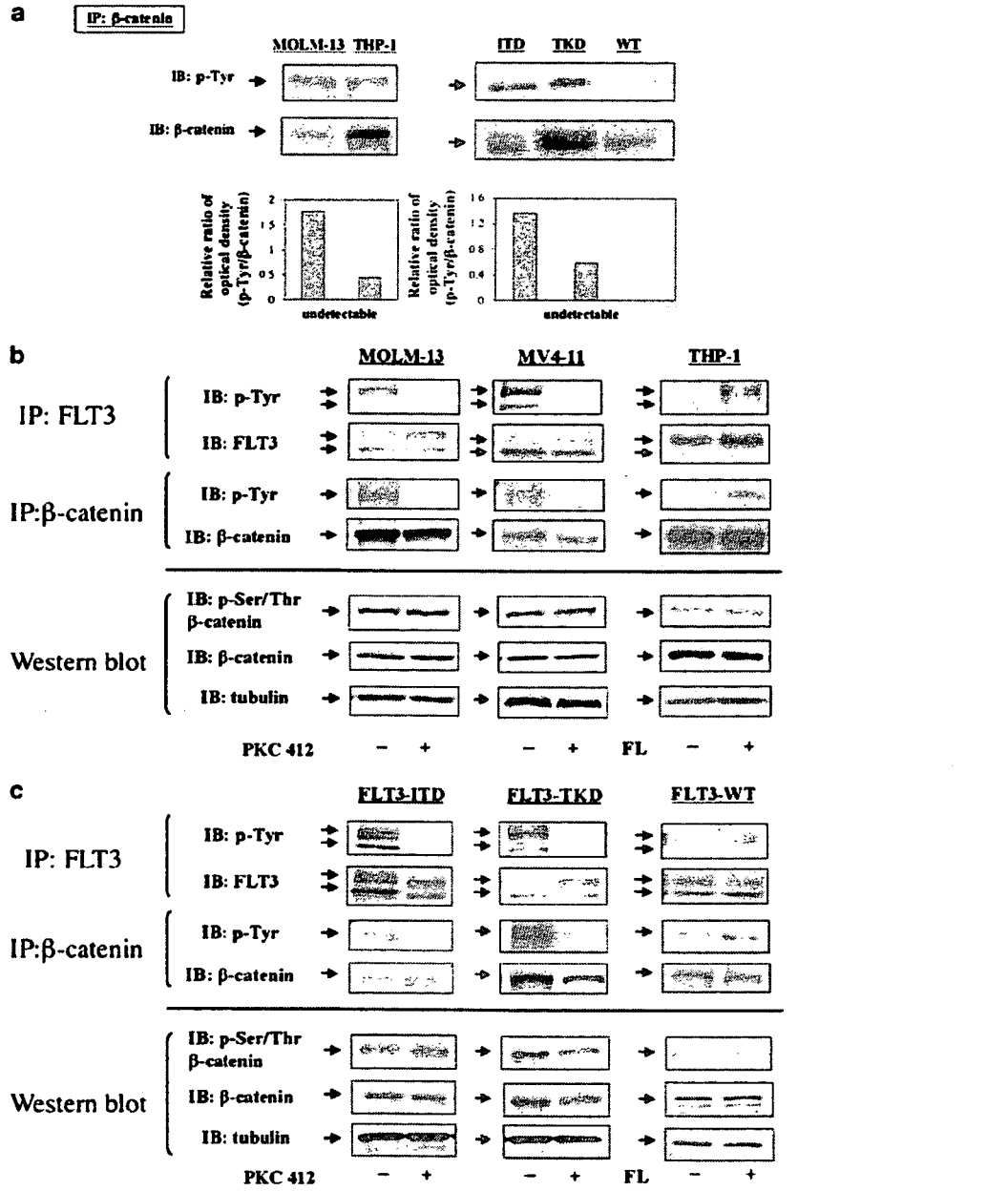

Figure 1 Tyrosine phosphorylation of β-catenin in FLT-3-expressing cell lines. (a) Cell lysates were obtained as described in 'Materials and methods'. To detect tyrosine phosphorylation of β-catenin, 1 mg of proteins from cell lysates was precipitated using 2 µg of anti-β-catenin antibody. Proteins were resolved by reducing 10% SDS-PAGE, electrotransferred to PVDF membrane and western blotted for anti-phosphotyrosine (upper panel). Membranes were stripped and reprobed with anti-β-catenin antibody (middle panel). Optical density ratio of phosphotyrosine/total β-catenin was measured using a GS-800 densitometer with Quantity One software (lower panel). (**b**, **c**) Effect of FLT3 inhibition or activation on β-catenin tyrosine phosphorylation. Cells were treated with or without PKC412 (20 nM for 2 h) or FLT3 ligand (FL; 50 ng ml^{-1} for 1 h) and then lysed. Protein (1 mg) from cell lysates was precipitated with 2 µg of anti-β-catenin antibody or 1.5 µg of anti-FLT3 antibody. Whole-cell lysates and immunoprecipitated samples were resolved by reducing 7.5% SDS-PAGE, electrotransferred to a PVDF membrane and western blotted with corresponding antibodies.

protocol. All patients gave informed consent according to the Declaration of Helsinki. Four individual cryopreserved AML samples, each harboring an FLT3-ITD mutation, were thawed in warm RPMI medium supplemented with 10% FBS and penicillin/streptomycin. After overnight incubation at 37 °C and 5% CO_2, samples were treated for 5 min with DNAse I (150 U ml^{-1}, Amersham) and subjected to centrifugation on Ficoll–Hypaque (Amersham) to remove necrotic cells. Eighty million cells from each sample were split into two aliquots. To one aliquot was added CEP-701 to a final concentration of 50 nM (FLT3 inhibited), while the other aliquot contained dimethylsulfoxide (DMSO) (control). After incubation at 37 °C, cells were divided into two aliquots, pelleted, lysed and immunoprecipitated for either FLT3 or β-catenin. Statistical analysis was performed using StatView software (SAS, Cary, NC, USA).

Results

Tyrosine phosphorylation of β-catenin is increased in activated FLT3-expressing AML cells

Tyrosine phosphorylation of β-catenin in FLT3-expressing cell lines was investigated by immunoprecipitation assay. As shown in Figure 1a (left panel), β-catenin in the FLT3-ITD cell line, MOLM-13, was more tyrosine-phosphorylated compared to a FLT3-WT cell line, THP-1. The phosphotyrosine/total β-catenin ratio was 3.75-fold greater in the FLT3-ITD-expressing cells than in the FLT3-WT-expressing cells. Similarly, using 32D transfectants (Figure 1a, right panel), β-catenin was more tyrosine-phosphorylated in cells expressing the activated FLT3 mutants FLT3-ITD and FLT3-TKD-32D, than in FLT3-WT transfectants.

To confirm the importance of FLT3 activation for tyrosine phosphorylation of β-catenin, we treated the cell lines with the FLT3 kinase inhibitor PKC412, which effectively inhibits the constitutive kinase activity of FLT3-ITD and FLT3-TKD[36,37] and the kinase activity stimulated by FLT ligand (FL). In the FLT3-ITD cell lines MOLM-13 and MV 4-11, treatment with PKC412 (20 nM for 2 h) decreased tyrosine phosphorylation of both FLT3 and β-catenin. Similar results were obtained with the FLT3 inhibitor AG1296 (data not shown). Conversely, FL (50 ng ml^{-1} for 1 h) induced tyrosine phosphorylation of FLT3 and β-catenin in THP-1 cells (Figure 1b, upper panel). In these settings, little change was observed in the total protein level of β-catenin and in its serine/threonine-phosphorylation status (Figure 1b, lower panel). In addition, PKC412 decreased tyrosine phosphorylation of FLT3 and β-catenin in FLT3-ITD-32D and FLT3-TKD-32D and FL increased phosphorylation of FLT3 and β-catenin in FLT3-WT-32D cells (Figure 1c, upper panel). As in the AML cell lines,

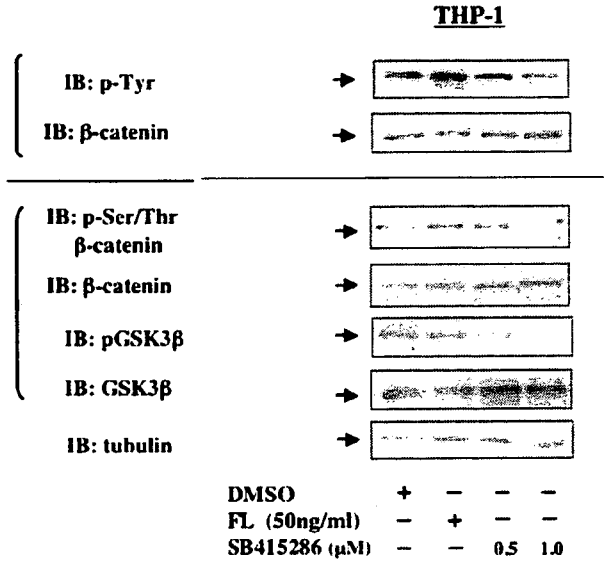

Figure 2 FLT3 regulates tyrosine phosphorylation of β-catenin. Effect of GSK3β inhibitor on total and tyrosine phosphorylation level of β-catenin. Cells were pretreated with or without SB415286 (0.5 or 1.0 μM for 3 h), then treated with FL (50 ng ml^{-1}) for 2 h. Because SB415286 was dissolved in DMSO, the same amount (0.1% final concentration) of DMSO was added to control cells. Preparation of cell lysates, immunoprecipitation and western blot are described in Materials and methods.

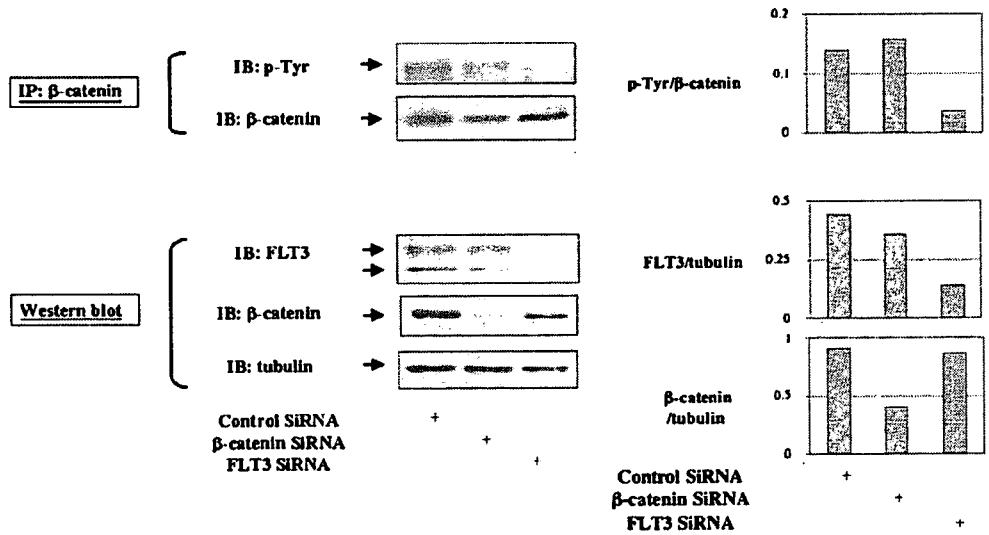

Figure 3 Silencing of FLT3 leads to reduced tyrosine phosphorylation of β-catenin. MOLM-13 cells were transfected with FLT3 siRNA, β-catenin siRNA or control siRNA. Following transfection, cells were incubated for 48 h. After incubation, cells were lysed and subjected to immunoprecipitation and immunoblotting assay. Optical density ratios were obtained using a GS-800 densitometer with Quantity One software.

no change was found in either the total level or phosphoserine/threonine status of β-catenin in 32D transfectants (Figure 1c, lower panel). These results suggest that tyrosine phosphorylation of β-catenin, not its serine/threonine phosphorylation or total level, closely parallels FLT3 activation status.

Stabilization of β-catenin following GSK3β inhibition does not promote enhanced tyrosine phosphorylation of β-catenin

To study the relationship between the tyrosine phosphorylation and the total level of β-catenin further, we investigated the effect of GSK3β inhibition on β-catenin tyrosine phosphorylation status. As shown in Figure 2, treatment with the GSK3β inhibitor SB415286 increased the total β-catenin level in THP-1 cell line and decreased β-catenin serine/threonine phosphorylation. However, SB415286 did not increase tyrosine phosphorylation of β-catenin in these cells, rather it decreased the ratio of tyrosine-phosphorylated/total β-catenin.

Silencing of FLT3 gene expression leads to reduced phosphorylation of β-catenin in FLT3-ITD AML cells

We next investigated whether RNAi-mediated knockdown of FLT3 expression affected β-catenin tyrosine phosphorylation similarly to small-molecule FLT3 kinase inhibitors. As shown in Figure 3, when the expression of FLT3 in MOLM-13 cells was suppressed with FLT3 siRNA, tyrosine phosphorylation of β-catenin was concomitantly reduced, while the total protein level of β-catenin was not changed. In contrast, while the protein level of β-catenin was suppressed by β-catenin siRNA, the ratio of tyrosine-phosphorylated/total β-catenin was not significantly affected.

Nuclear localization of β-catenin in activated FLT3-expressing cell lines

Because tyrosine phosphorylation of β-catenin has been reported to be associated with increased nuclear accumulation,[25,33,38] we investigated the subcellular localization of β-catenin by immunocytochemistry and western blot. Although β-catenin was located mainly in the cytoplasm in THP-1, it was primarily nuclear in MOLM-13 (Figures 4a and b). After treatment with PKC412, the amount of nuclear β-catenin was markedly decreased in MOLM-13 cells. Similar to PKC412 treatment, FLT3 siRNA decreased nuclear β-catenin while control siRNA had no effect. In contrast, after treatment of THP-1 cells with FL, the amount of nuclear β-catenin was increased. Western blotting of subcellular fractions confirmed β-catenin to be enriched in the nuclear fraction of cells with active FLT3 signaling (Figure 4c). These findings suggest that activated FLT3 is associated with increased nuclear accumulation of β-catenin and that nuclear β-catenin is preferentially tyrosine-phosphorylated.

Activation status of FLT3 affects β-catenin target gene expression in AML and 32D cell lines

Because enhanced nuclear localization of β-catenin was correlated with the activation status of FLT3, we wished to determine whether β-catenin-dependent transcription could be affected by FLT3 activity in MOLM-13, THP-1 and 32D transfectants. To examine this question, the mRNA levels of two β-catenin target genes, cyclin D1 and c-*myc*, were measured using real-time RT-PCR. In cells with FLT3 gain-of-function mutations, PKC412 treatment markedly decreased RNA expression of both c-*myc* and cyclin D1 (Figure 5a). In cells with

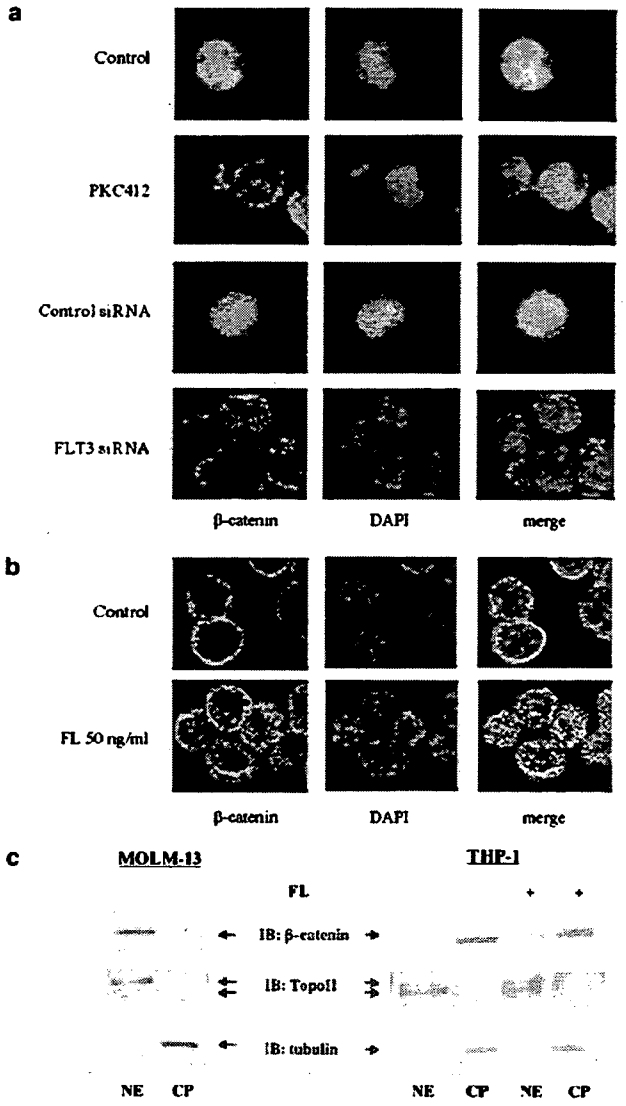

Figure 4 Nuclear localization of β-catenin in activated FLT3 cell lines. (**a**, **b**) MOLM-13 (**a**) and THP-1 (**b**) cells were treated with or without PKC412 (20 nM for 2 h), control siRNA (48 h), FLT3 siRNA (48 h) or FL (50 ng ml^{-1} for 30 min) and then were cytocentrifuged. Cells were fixed in 3.7% formaldehyde/PBS and permeabilized with 0.2% Triton X-100. β-Catenin was visualized by immunofluorescence (green, left panel). The DNA-intercalating dye DAPI was used to identify cell nuclei (blue, center panel). The right panel presents a merged image to highlight the nuclear pool of β-catenin. To facilitate visualization of the nuclear localization of β-catenin in THP-1, the green/blue merged signal was converted to violet by the image analysis software. Images were collected using a ×100 objective. (**c**) Western blot analysis of β-catenin in subcellular fractions. Preparation of subcellular fractions is described in Materials and methods. To verify the purity of subcellular fractions and to control for protein loading, blots were reprobed with antibodies to topoisomerase II (Topo II) for nuclear fractions and α-tubulin (tubulin) for cytoplasmic fractions.

FLT3-WT, expression of c-*myc* and cyclin D1 was increased after treatment with FL (suggesting functional nuclear localization of β-catenin), while SB415286 had very little effect (Figure 5b). Similar to PKC412 treatment, FLT3 siRNA decreased expression of cyclin D1, as did β-catenin siRNA (Figure 5c).

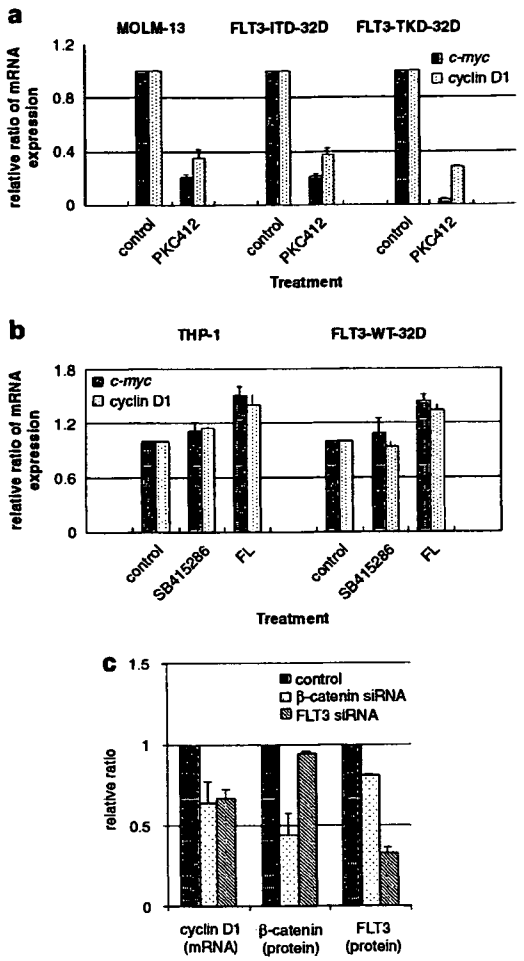

Figure 5 Effect of FLT3 activation on β-catenin target gene expression in AML cell lines. (a, b) Cells were treated as follows: 0.1% DMSO (control), 20 nM PKC412 for 4 h (PKC412) or 50 ng ml^{-1} FL for 4 h (FL). Total RNA was isolated from the cells and quantitative RT-PCR was performed in duplicate. All samples were normalized to the level of 18S ribosomal RNA. The mean of two individual experiments and standard deviations are shown. (c) MOLM-13 cells were transfected with indicated siRNA. After 48 h, total RNA was isolated and quantitative RT-PCR was performed as described.

Active FLT3 binds to β-catenin

We used co-immunoprecipitation techniques to investigate the possible physical interaction between FLT3 and β-catenin. In MOLM-13 cells, endogenous β-catenin co-immunoprecipitated with endogenous FLT3. This association was markedly reduced in cells treated with PKC412 (Figure 6a). In the reciprocal experiment, FLT3 was co-immunoprecipitated by anti-β-catenin antibody in untreated cells, but this association was reduced in PKC412-treated cells (Figure 6b). In THP-1 cells, although a small amount of β-catenin was co-immunoprecipitated with anti-FLT3 antibody in the absence of FL, the proportion of β-catenin bound to FLT3 was increased after FL treatment (Figure 6a). This observation was confirmed by co-immunoprecipitation with anti-β-catenin antibody (Figure 6b). These results demonstrate that active FLT3 preferentially binds to β-catenin, whether the kinase is mutated or not, and that inhibition of FLT3 activation decreases interaction between FLT3 and β-catenin.

Active FLT3 kinase phosphorylates β-catenin directly

To determine whether active FLT3 can directly phosphorylate tyrosine residues of β-catenin, we performed an *in vitro* kinase assay using recombinant active FLT3 as enzyme source and recombinant β-catenin as substrate. As shown in Figure 6c, no tyrosine phosphorylation of β-catenin was detected in the absence of FLT3 protein (upper panel, lane 2). Addition of active FLT3 kinase induced tyrosine phosphorylation of β-catenin, while inclusion with the FLT3 inhibitor AG1296 decreased tyrosine phosphorylation of both FLT3 and β-catenin (upper panel, lanes 3 and 4). These results suggest that active FLT3 kinase can directly phosphorylate tyrosine residues of β-catenin.

Tyrosine phosphorylation of β-catenin in mononuclear cells obtained from FLT3-ITD-positive AML patients is suppressed by the FLT3 inhibitor CEP-701

To determine whether these observations are of clinical relevance, we investigated the effect of FLT3 inhibition on the tyrosine phosphorylation status of β-catenin in mononuclear cells of AML patients. Four individual isolates of bone marrow mononuclear cells obtained from patients harboring the FLT3-ITD mutation were treated *ex vivo* with the FLT3 inhibitor CEP-701 (50 nM). As shown in Figure 7, this treatment markedly reduced the level of FLT3 phosphorylation ($P=0.0046$). In each case, tyrosine phosphorylation of β-catenin was concomitantly reduced in a time-dependent manner ($P=0.043$).

Discussion

Wnt signaling is required for normal hematopoiesis, and deregulated Wnt signaling has been implicated in the etiology and progression of several hematologic malignancies.[27–31] Wnt effector β-catenin is expressed in both lymphoid and myeloid leukemia cell lines and primary cells. Inhibition of Wnt/β-catenin signaling in Jurkat T-lymphoblastic cells impaired proliferation and increased susceptibility to apoptosis in response to Fas ligation.[28] In multiple myeloma (MM), β-catenin protein was found to be overexpressed, and stimulation by various Wnts led to its accumulation and nuclear translocation accompanied by cell proliferation.[29] In colorectal cancer, truncation or loss of the APC protein, or mutation of the GSK-3β phosphorylation sites in β-catenin, is thought to be critical mechanism underlying β-catenin cytoplasmic and nuclear accumulation, promoting the expression of β-catenin-regulated pro-proliferative and survival genes.[20,39] However, Wnt signaling was reported to be increased in AML and MM without mutation of APC or β-catenin,[29,31] suggesting that alternative mechanisms might contribute to β-catenin deregulation in hematologic malignancies. Recently, Wnt-independent signaling has been suggested to cooperate with FLT3 in myeloid transformation. Protein expression and activity of β-catenin in fostering TCF/LEF-dependent transcription were increased in FLT3-ITD-32D cells independent of extracellular Wnt ligand.[32] However, the mechanism underlying this phenomenon has remained unclear.

Tyrosine phosphorylation of β-catenin has been studied not only for its impact on the physical association between β-catenin and E-cadherin but also for its relationship to β-catenin-dependent TCF transcriptional activity. Phosphorylation of Tyr-142 and Tyr-654 on β-catenin promotes its release from E-cadherin and its accumulation in the cytoplasm.[25,40,41] Since β-catenin has been shown to freely equilibrate between the